

REPORT DOCUMENTATION PAGE

1a. REPORT SECURITY CLASSIFICATION UNCLASSIFIED		1b. RESTRICTIVE MARKINGS	
2a. SECURITY CLASSIFICATION AUTHORITY		3. DISTRIBUTION / AVAILABILITY OF REPORT Approved for public release; distribution is unlimited.	
2b. DECLASSIFICATION / DOWNGRADING SCHEDULE			
4. PERFORMING ORGANIZATION REPORT NUMBER(S)		5. MONITORING ORGANIZATION REPORT NUMBER(S) AFOSR-TR-89-110	
6a. NAME OF PERFORMING ORGANIZATION Catholic University of America	6b. OFFICE SYMBOL (If applicable)	7a. NAME OF MONITORING ORGANIZATION AFOSR/NP	
6c. ADDRESS (City, State, and ZIP Code) P.O. Box 657, Cardinal Station Washington, DC 20064		7b. ADDRESS (City, State, and ZIP Code) Building 410, Bolling AFB DC 20332-6448	
8a. NAME OF FUNDING / SPONSORING ORGANIZATION AFOSR	8b. OFFICE SYMBOL (If applicable) NP	9. PROCUREMENT INSTRUMENT IDENTIFICATION NUMBER AFOSR-86-0160	
8c. ADDRESS (City, State, and ZIP Code) Building 410, Bolling AFB DC 20332-6448		10. SOURCE OF FUNDING NUMBERS	
		PROGRAM ELEMENT NO. 61102F	TASK NO. 2311
		WORK UNIT ACCESSION NO. A1	
11. TITLE (Include Security Classification) (U) MHD SLOW SHOCKS IN CORONAL AND INTERPLANETARY SPACE			
12. PERSONAL AUTHOR(S) Dr Y C Whang			
13a. TYPE OF REPORT FINAL	13b. TIME COVERED FROM 1 Jun 86 to 31 May 89	14. DATE OF REPORT (Year, Month, Day) Aug 1989	15. PAGE COUNT 33
16. SUPPLEMENTARY NOTATION			
17. COSATI CODES		18. SUBJECT TERMS (Continue on reverse if necessary and identify by block number)	
FIELD	GROUP	SUB-GROUP	
	04.01		
19. ABSTRACT (Continue on reverse if necessary and identify by block number) <p>The overall objective of this project is to study shock waves of the solar terrestrial medium in coronal and interplanetary space. This research will enhance our understanding on the propagation of large amplitude disturbances from the solar corona through the interplanetary space. The work accomplished during the past three years includes:</p> <ul style="list-style-type: none">(a) a demonstrating example showing the formation of slow shock pairs associated with CMEs in a coronal environment;(b) a parametric study of slow shocks in the entire domain of a three-dimensional parameter space, the A, θ, β-space;(c) the large scale geometry of traveling interplanetary shocks;(d) the transition of slow shocks to fast shocks in the inner solar wind; and(e) the evolution of CME associated shocks and their interplanetary manifestations.			
20. DISTRIBUTION / AVAILABILITY OF ABSTRACT <input checked="" type="checkbox"/> UNCLASSIFIED/UNLIMITED <input type="checkbox"/> SAME AS RPT <input type="checkbox"/> DTIC USERS		21. ABSTRACT SECURITY CLASSIFICATION UNCLASSIFIED	
22a. NAME OF RESPONSIBLE INDIVIDUAL H R RADOSKI		22b. TELEPHONE (Include Area Code) (202) 767-4906	22c. OFFICE SYMBOL AFOSR/NP

DTIC FILE COPY

✓ (2)

The Catholic University of America, Washington, DC 20064

Submitted to

Air Force Office of Scientific Research
Bolling Air Force Base, Washington DC 20332

Final
~~Interim~~ report

For Research project Entitled

MHD SLOW SHOCKS IN CORONAL AND INTERPLANETARY SPACE

Grant No: AFOSR-086-0160

Period: From June 1, 1986 to May 31, 1989

Program Manager: Dr. Henry R. Radoski
NP (202) 767-4906

Principal Investigator: Yun Chow Whang (SSN: 470-50-6730)
Dept. Mechanical Engineering
The Catholic University of America
Washington, D.C. 20064
Phone number: 202-635-5170

AD-A214 725

Y C Whang
Yun Chow Whang, Professor
Principal Investigator

DTIC
ELECTE
NOV 20 1989
S B D

1. Summary

The overall objective of this project is to study shock waves of the solar terrestrial medium in coronal and interplanetary space. These shocks are magnetohydrodynamic (MHD) slow shocks and fast shocks. Our primary interests are to study dynamic problems related to shocks associated with coronal mass ejections (CMEs), including the formation of shocks in coronal environment, the transition of slow shocks to fast shocks, their evolution and their interaction with the solar wind in coronal and interplanetary space.

During the past three years of this grant, we have produced the following publications :

[Paper 1] Whang, Y. C., Slow Shocks and Their Transition to Fast Shocks in the Inner Solar Wind, J. Geophys. Res., 92, 4349-4356 (1987).

[Paper 2] Whang, Y. C., Evolution of Interplanetary Slow Shocks, J. Geophys. Res., 93, 251-255 (1988).

[Paper 3] Whang, Y. C., Forward-Reverse Shock Pairs Associated with Coronal Mass Ejections, J. Geophys. Res., 93, 5897-5902 (1988).

[Paper 4] Whang, Y. C., CME Associated Forward-Reverse Shock Pairs, Adv. Space Res., 9, (4)81-86, (1989).

[Paper 5] Whang, Y. C., Formation of Slow Shock Pairs Associated With Coronal Mass Ejections, in press, in the Proceedings of the Chapman Conference on the Physics of Magnetic Flux Ropes, AGU Publication (1989).

In the following sections, we summarize some highlights of these studies.

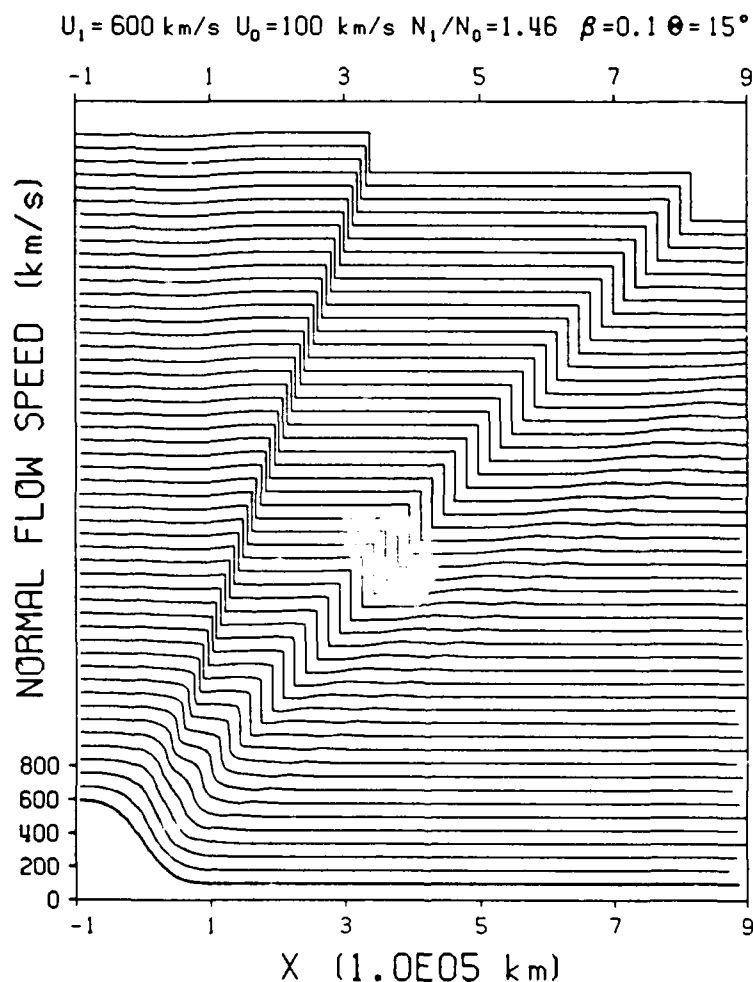
2. Formation of Slow Shock Pairs Associated With CMEs

In order to understand the basic physics involved in the shock formation process, we carry out a series of MHD simulations to show that MHD shocks formed in low-beta plasmas in the coronal environment are slow shocks. The simulation model assumes that flow properties are functions of x and t only. The x -direction is normal to the wave front in the forward direction of the solar wind flow and the magnetic field vector is parallel to the xy coordinate plane. The time-dependent MHD flow governed by a system of hyperbolic, nonlinear equations is studied using the method of characteristics. Shocks are treated as surfaces of zero thickness. The Rankine-Hugoniot solution is used to calculate the jumps in flow properties at all shock crossings.

The numerical solution shown in Figure 1 demonstrates the formation of a forward-reverse slow shock pair in a coronal environment. The initial condition represents the impact of a high-speed (600 km/s) mass ejecta on a low-speed (100 km/s) ambient solar wind. At $t = 0$ the flow velocity changes smoothly over a distance of about 200,000 km. On the upstream (mass ejecta) side $U_1 = 600$ km/s and $n_1 = 8.8 \times 10^6$ protons/cm³. On the downstream (ambient solar wind) side, $U_0 = 100$ km/s and $n_0 = 6.0 \times 10^6$ protons/cm³. The flow is field aligned in the rest frame of reference, $\beta = 0.1$, $B_x = 0.8$ Gauss, and $\theta = 15^\circ$.

The simulation demonstrates that the difference in momentum flux is the driving force for the formation of shock pairs. The momentum impact compresses the plasma near the front of the CME. Large pressure disturbances propagate in both the forward direction relative to the ambient solar wind and the reverse direction relative to the ejecta flow. The pressure fronts steepen to form forward and reverse MHD shocks. The flow speed profiles calculated at a time interval of 30 seconds (Figure 1) show the gradual formation of the two shock fronts. The resulting shocks consist of a forward slow shock and a reverse slow shock. No fast shocks. The shock pair takes about 10 minutes to grow into a fully developed state.

The disturbances generated by the momentum impact also disturb the flow field outside the interaction region bounded by the forward-reverse slow shock pair. But their influence is limited to the region bounded by a forward fast mode characteristic on the downstream side and by a reverse fast mode characteristics on the upstream side. The amplitudes of disturbances outside the slow shocks are negligibly small compared with jumps in flow properties across the slow shocks.



Accession For	
NTIS GRA&I	<input checked="" type="checkbox"/>
DTIC TAB	<input type="checkbox"/>
Unannounced	<input type="checkbox"/>
Justification	
By	
Distribution/	
Availability Codes	
Dist	Avail and/or Special
A-1	

Fig. 1. The flow speed profiles calculated at a time interval of 30 seconds showing the gradual formation of the two shock fronts.

3. A Parametric Survey of MHD Slow Shocks

We have an exact analytical method to calculate the solutions of MHD shocks as functions of three dimensionless upstream parameters: the shock Alfvén number $A = U_n / (a \cos \theta)$, the shock angle θ , and the plasma β value. (Here U_n is the normal component of the relative shock speed, a the Alfvén speed, θ the acute angle between the shock normal and the magnetic field, and β the ratio of the thermal pressure p to the magnetic pressure $B^2/8\pi$.) A shock is a slow shock if the shock Alfvén number A is less than 1 and is a fast shock if A is greater than 1. The magnetic field and the shock angle decrease across a slow shock, they increase across a fast shock.

The parametric survey of slow shock solutions are presented in a three dimensional A, θ, β -space. The domain of slow shock solutions in the A, θ -parameter space shrinks as the plasma β value decreases. A drastic change in the domain of solution takes place when β is between 0.1 and 1. The change becomes very small at very large or very small β . When the shock Alfvén number approaches one, slow shocks exist at all shock angles and at all β values. At any given value of β , a whole range of changes in B_2/B_1 , from 0 to 1, may take place. On the other hand the range of change in thermodynamic properties strongly depends on the β value. In Figure 2 of Paper 2 shows the density ratio, ρ_2/ρ_1 , in the three dimensional A, θ, β -parameter space. (A similar plot has been made for the pressure ratio.) Slow shocks covering a wide range of density jumps exist in the low β region (where $\beta \leq 0.1$). On the other hand, only slow shocks with weak density jumps exist in the high β region (where $\beta \geq 1$). Therefore, in the coronal space where the β value of the solar wind is in the order of 0.1, all physical properties may jump across a slow shock over a wide range of magnitudes. Near 1 AU the plasma β value is in the order of 1, the jumps in thermodynamic properties across a slow shock must be small but the change in the magnetic field is not necessarily small.

4. Transition of Slow Shocks to Fast Shocks

Whang [Paper 1] first studied the possible existence of forward slow shocks preceding some CMEs and their global geometry. When the speed of ejected CME material relative to the ambient solar wind exceeds the local magnetoacoustic speed, an MHD shock front forms at the leading edge of the compressed ambient plasma shell. In coronal space, the Alfvén speed is of the order of 1000 km/s. If a forward MHD shock forms preceding the compressed ambient plasma shell associated with the CME, the shock Alfvén number can be less than 1 and the shock can be a forward slow shock. The large-scale global surface of a forward slow shock should have a bow-shaped surface with its nose facing the sun because the slow-mode MHD waves and MHD shocks are upstream-inclined [Sears and Resler, 1961]. The relative shock speed varies from point to point on the curved surface of an MHD shock. The slow shock is relatively stronger at the nose. The shock becomes weaker on the flank and asymptotically approaches slow-mode MHD waves.

Sheeley et al. [1985] have demonstrated a close association between interplanetary shocks and CMEs. They reported that with very few exceptions interplanetary shocks detected at Helios A are produced by CMEs observed from Solwind coronagraph. Richter et al. [1985] reported a very certain identification of a forward slow shock at 0.31 AU. Hundhausen et al. [1987] studied CMEs observed from the coronagraphs aboard Skylab and on the Solar

Maximum Mission satellite. The observed flattening of the tops of some mass ejection loops suggests the possible existence of traveling forward slow shocks immediately in front of some CMEs. The observed speeds for the outward motion of CMEs show that the speed at which a CME is overtaking the ambient coronal plasma is less than the Alfvén speed but greater than the sound speed for many (probably most) observed CMEs. This supports the possible existence of forward slow shocks.

The Alfvén speed of the interplanetary plasma decreases at increasing heliocentric distance in the inner solar wind. As a forward slow shock travels outwards from the sun, the decrease in the Alfvén speed causes the shock Alfvén number of a forward slow shock to become greater than 1 at increasing heliocentric distances and the shock evolves from a slow shock into a fast shock. The large-scale global surface of a traveling forward fast shock has a bow-shaped surface with its nose facing away from the sun.

Wang [Paper 1] has a theory to explain the transition of traveling slow shocks into traveling fast shocks as shown in Figure 6 of Paper 1. The Alfvén speed of the interplanetary plasma decreases at increasing heliocentric distance in the inner solar wind. As the forward slow shock moves outwards from the sun, the decrease in the Alfvén speed causes the shock Alfvén number to reach 1 near the nose of the shock surface, the transition from a forward slow shock to a forward fast shock begins to take place at a point of the shock surface where the shock angle equals 0° . The onset of transition must occur in the region of interplanetary space where $\beta < 2/\gamma$ or 1.2. At the onset of the transition the forward slow shock smoothly converts to a system consisting of a forward slow shock, a very weak forward rotational discontinuity (an Alfvén wave), and a very weak forward fast shock (a fast MHD wave).

During the transition, the system consists of a slow shock, a fast shock, and a rotational discontinuity. The three surfaces of discontinuity intersect along a closed transition line. As the system moves outward from the sun the transition line moves laterally across the field lines. The area enclosed by the closed loop of the transition line expands continuously, the fast shock grows stronger, and the slow shock becomes weaker. Eventually, the slow shock diminishes and the entire system evolves into a forward fast shock. Such a system may have been observed from ISEE 1 and 3. Kennel et al. [1984a, b] reported that on November 12, 1978, ISEE 1 and 3 observed a forward fast shock associated with a pair of flares which occurred some 48 hours earlier. The shock was followed by a strong rotational discontinuity at approximately $40 R_E$ downstream of the shock. This sequence of events resembles the forward transition system.

5. Evolution of CME Associated Shock Pairs

Recently, Wang [Paper 3] suggests that for some CMEs their interaction with the ambient solar wind can produce a forward-reverse shock pair as shown in Figure 1 of Paper 3. We may call the ejected material the CME plasma which is separated from the solar wind plasma in the background corona by an interface. The large momentum of the high-speed mass ejecta exerts an excessive pressure on the ambient plasma shell in a narrow region in front of the CME. The high-speed mass ejecta causes a sudden increase in the pressure of the plasma near the top of the CME on both sides of the interface.

In response to the large pressure in the compressed ambient plasma shell, the CME plasma immediately behind the interface is decelerated, compressed and heated. This compressed CME plasma is confined in a narrow region bounded by the interface on the forward side and by a pressure front on the reverse side. The front of the compressed CME plasma propagates in the reverse direction relative to the ejecta flow, it may steepen to form a reverse shock.

The ejected CME plasma carrying a strong magnetic field is a low- β plasma in which the slow mode magnetoacoustic speed C_s is much less than the Alfvén speed a . The reverse shock associated with CME can be a slow shock if the normal component of the relative shock speed U_n is greater than C_s but less than $a \cos \theta$. Whang estimated that the reverse shock can be a slow shock whether the forward one is a slow-mode or a fast-mode shock. As a slow shock pair travels outward from the Sun, the decrease in the Alfvén speed with increasing heliocentric distance causes the slow shocks to evolve into fast shocks.

MacQueen [1980] suggested that CMEs do not carry out distended field very far to interplanetary space, but rather are subject to a reconnection process. He proposed that CME loops must magnetically disconnect from the sun and form a closed magnetic structure.

Burlaga et al. [1981] analyzed the magnetic field configuration behind three shocks. They found a systematic configuration of the magnetic field and called it the magnetic cloud. Klein and Burlaga [1982] identified 45 clouds in interplanetary data obtained near 1 AU between 1967 and 1978. They compared the physical properties of magnetic clouds with those of CMEs and suggested an association of some clouds with disconnected magnetic structures of CMEs. They identified a magnetic cloud as an interplanetary structure in which the magnetic field strength is higher than average, the magnetic field direction rotates monotonically through a large angle, the temperature is low, and the plasma β is significantly lower than 1. A good case of an association between a CME observed by Solwind and a magnetic cloud observed at 0.54 AU by Helios 1 two days later was presented by Burlaga et al. [1982].

In summary, two important evolutions of the shock pairs associated with CMEs may occur in interplanetary space. First, a CME loop eventually disconnect from the sun to form a closed magnetic structure. The disconnected bubble manifests as a magnetic cloud in interplanetary space. Second, as the CME associated forward-reverse shock pair moves outwards in interplanetary space, they evolve into a pair of fast shocks. The reverse shock first propagates within the magnetic cloud, but eventually the reverse shock must exit the cloud to become detached from the magnetic cloud. Then both the forward and the reverse shocks propagate in the ambient solar wind. Therefore, the interplanetary consequence of some CMEs should consist of a magnetic cloud accompanied by a fast shock pair. The forward fast shock propagates preceding the cloud and the reverse fast shock is either within or behind the cloud.

Klein and Burlaga [1982] reported that about one third of clouds identified near 1 AU between 1967 and 1978 are preceded by a shock. There are several examples involving the observation of a shock pair associated with a CME or magnetic cloud. Lepping et al. [1988] reported that a large magnetic cloud accompanied by a shock pair was observed on October 31 and November 1 of 1972 from IMP 7. The event was associated with a unusually longlasting solar flare

which occurred some 49 hours earlier. Gosling et al. [1988] have identified two CME associated shock pairs at 1 AU from ISEE 3. Another event involving a shock pair and a magnetic cloud was observed on August, 1982, from Voyager 2 at 10.3 AU [Burlaga et al., 1985]. This observation shows that for a long-lived cloud, the reverse shock had enough time to propagate through the cloud, exited the rear of the cloud, and appeared closely behind the cloud.

SLOW SHOCKS AND THEIR TRANSITION TO FAST SHOCKS IN THE INNER SOLAR WIND

Y. C. Whang

Department of Mechanical Engineering, Catholic University of America, Washington, D. C.

Abstract. The jump conditions of MHD shocks may be directly calculated as functions of three upstream conditions: the shock Alfvén number based on the normal component of the relative shock speed, the shock angle, and the plasma β value. The shock Alfvén number is less than 1 for a slow shock and greater than 1 for a fast shock. A traveling, forward shock can be a slow shock in coronal space, where the Alfvén speed is of the order of 1000 km/s. The surface of a forward slow shock has a bow-shaped geometry with its nose facing toward the sun. The decrease in the Alfvén speed at increasing heliocentric distance causes the shock Alfvén number of a forward slow shock to become greater than 1, and the shock eventually evolves from a slow shock into a fast shock. During the transition the shock system consists of a slow shock, a fast shock, and a rotational discontinuity. They intersect along a closed transition line. As the system moves outward from the sun, the area enclosed by the transition line expands, the fast shock grows stronger, and the slow shock becomes weaker. Eventually, the slow shock diminishes, and the entire shock system evolves into a forward fast shock.

1. Introduction

Interplanetary traveling shocks are associated with corona mass ejections and flares [Dryer 1975; Hildner, 1977; MacQueen, 1980; Sheeley et al., 1985]. If the speed of the ejected material relative to the ambient solar wind exceeds the local magnetoacoustic speed, a magnetohydrodynamic (MHD) shock front forms at the leading edge of the compressed ambient plasma shell. The MHD shock process plays an important role in influencing solar terrestrial relations.

The solutions of MHD shocks may be expressed as functions of three upstream conditions: the shock Alfvén number based on the relative shock speed $A = U_n / (a \cos \theta)$, the shock angle θ , and the plasma β value. (Here U_n is the normal component of the relative shock speed, a the Alfvén speed, θ the acute angle between the shock normal and the magnetic field, and β the ratio of the thermal pressure p to the magnetic pressure $B^2/8\pi$.) Two kinds of MHD shocks, the fast and the slow shocks, may exist. A shock is a slow shock if the shock Alfvén number A is less than 1 and is a fast shock if A is greater than 1.

A traveling, forward MHD shock can be a slow shock in coronal space where the Alfvén speed is of the order of 1000 km/s. The Alfvén speed decreases at increasing heliocentric distance in the inner solar wind. The decrease in the Alfvén speed causes the shock Alfvén number of a forward

slow shock to become greater than 1 at increasing heliocentric distances, and the shock eventually evolves from a slow shock into a fast shock. A theoretical prediction for the global geometry of traveling slow shocks and their transition to fast shocks was first presented at 1986 Spring Meeting of the American Geophysical Union [Whang, 1986a]. Recently, we have carried out a numerical solution to demonstrate the transition process. This paper contains a formal presentation of these researches.

Theoretical investigations of MHD slow shocks in space plasma have been reported by Neubauer [1976], Rosenau and Suess [1977], Whang [1982, 1986a, b], Hada and Kennel [1985], and Edmiston and Kennel [1986]. Very few of the observed interplanetary shocks are slow shocks. Observations of interplanetary slow shocks near 1 AU have been reported by Chao and Olbert [1970] and by Burlaga and Chao [1971]. However, observations of slow shocks by Helios at a heliocentric distance of 0.31 AU [Richter et al., 1985] and by ISEE 3 beyond 100 earth's radii in the geomagnetic tail [Feldman et al., 1985] greatly increase our interest in slow shocks. A better understanding of the MHD slow shock process may have direct applications to the magnetic field reconnection process and to shock processes in coronal space, in interplanetary space, and in geomagnetic tails.

Recently, A. J. Hundhausen et al. (Do slow shocks precede some coronal mass ejection?, submitted to *Journal of Geophysical Research*, 1986) (hereafter referred to as HHL) studied the outward motion for coronal mass ejections observed by the Skylab coronagraph and the SMM coronagraph. The measured speeds of coronal mass ejections indicate that many mass ejections move into the background corona faster than the gasdynamic sound speed but slower than the Alfvén speed. This has been interpreted as a support for the possible formation of slow MHD shocks immediately in front of some coronal mass ejections.

2. Interplanetary Slow Shock and Its Transition to Fast Shock

Two kinds of MHD shocks, the fast and the slow shocks, may exist in coronal and interplanetary space. The plasma density, the thermal pressure, and the total pressure (the sum of the thermal and the magnetic pressures) all increase across an MHD shock. The magnetic field and the shock angle decrease across a slow shock and increase across a fast shock. The density ratio ρ_2/ρ_1 is often used as a measure of the shock strength. Here the subscript 1 denotes the flow condition upstream of a shock, and 2 denotes the flow condition downstream. Figures 1 and 2 show the constant contours for the density ratio and the magnetic field ratio for slow and fast shocks, respectively, as functions of three dimensionless

Copyright 1987 by the American Geophysical Union

Paper number 6A8720

0148-0227/87/006A-8720\$05.00

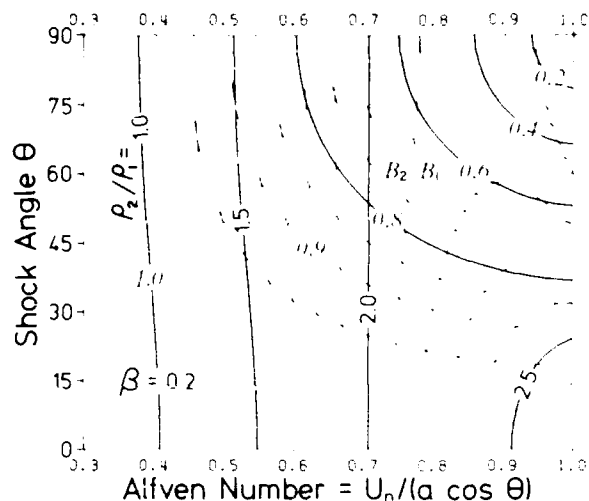


Fig. 1. The constant contours for the density ratio and the magnetic field ratio of slow shocks. The jump conditions of MHD shocks can be directly calculated as functions of three dimensionless upstream parameters: the shock Alfvén number $A = U_{n1} / (a_1 \cos \theta_1)$, the shock angle θ_1 , and β_1 . The magnitude of the magnetic field decreases across a slow shock.

upstream parameters: the shock Alfvén number $A = U_{n1} / (a_1 \cos \theta_1)$, the shock angle θ_1 , and β_1 .

In coronal space the Alfvén speed is of the order of 1000 km/s; an MHD shock in the inner solar wind is a slow shock if the shock Alfvén number A is less than 1. An interesting feature of interplanetary slow shocks is that the surface of a forward slow shock should have a bow-shaped surface with its nose facing the sun. The sketch on the left panel of Figure 3 shows the predicted geometry of a forward slow shock on the heliographic equator. The solar wind plasma enters a shock from its front side. The front side (the upstream side) of a forward shock is the side farther away from the sun and back side (the downstream side) is the side closer to the sun. An important characteristic of slow shocks (and slow MHD waves) is that they are upstream-inclined [Sears and Resler, 1961]. Therefore, looking at the forward slow shock from the sun, one sees the convex back side surface of the slow shock. The relative shock speed varies from point to point on the curved surface of an MHD shock. The slow shock is relatively stronger at the nose. The shock becomes weaker on the flank and asymptotically approaches to slow mode MHD waves. The shock angle θ decreases across the slow shock by a deflection angle δ . HHL pointed out that the upstream inclined nature of slow MHD shocks is relative to the magnetic field geometry; thus in a diverging radial background field, a large-scale traveling slow shock may have a rather flat configuration. They used the observed flattening of the tops of some mass ejection loops as they move outward through the corona to support the possible existence of traveling slow shocks.

In the inner heliosphere the Alfvén speed decreases at increasing heliocentric distance. As a forward slow shock travels outward from the sun, the decrease in the Alfvén speed causes the shock Alfvén number of a forward slow shock to reach 1 near the nose of the shock surface, and the transition from a slow shock to a fast shock

begins to take place. The shock angle $\theta = 0$ at the initial transition point. The onset of transition can occur in the region where $\beta \leq 2/\gamma$ or 1.2. Here γ is the ratio of specific heats. All calculations carried out in this paper use $\gamma = 5/3$ for a fully ionized plasma. Note that when $\beta = 2/\gamma$, the Alfvén speed equals the gasdynamic sound speed. When $\beta \leq 1.2$, the phase speed of the fast MHD wave equals the Alfvén speed at $\theta = 0$. The two plots in Figure 2 demonstrate that near $A = 1$, fast MHD shocks exist when $\beta \leq 1.2$ and but not when $\beta > 1.2$.

At greater heliocentric distances the forward slow shock may eventually evolve into a forward fast shock. Looking at a forward fast shock from the sun, the back side surface of the forward traveling fast shock is concave because the fast mode MHD waves and MHD shocks are downstream-inclined. Thus the large-scale global surface of a traveling forward fast shock has a bow-shaped surface with its nose facing away from the sun as shown in the right panel of Figure 3. The deflection angle of the magnetic field represents the increase of the shock angle across a fast shock.

During the transition the shock system consists of a slow shock, a fast shock, and a rotational discontinuity which may be referred to as a slow-fast shock system. We will continue to discuss the slow-fast shock system.

3. Jump Conditions of MHD Shocks

We obtain a direct and simple solution for the jump conditions of MHD oblique shocks. The jump

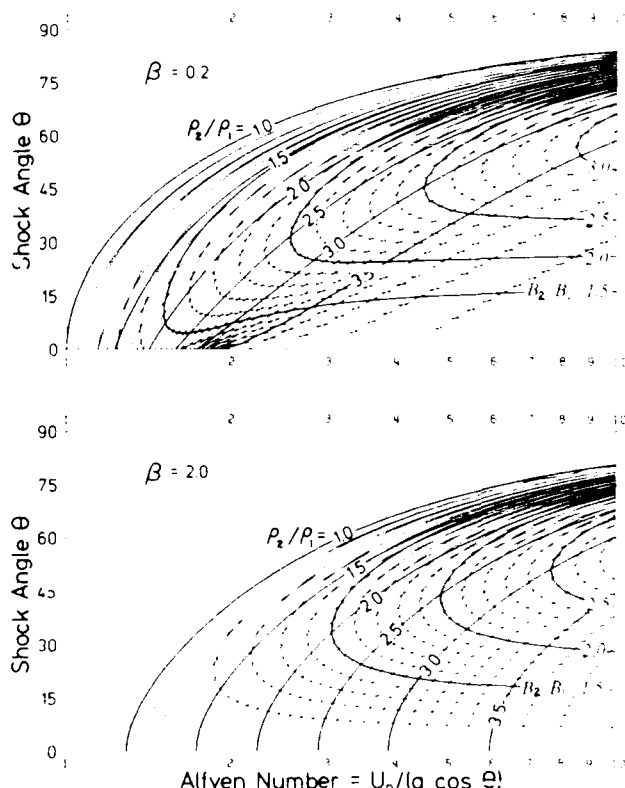


Fig. 2. The constant contours for the density ratio and the magnetic field ratio of fast shocks. The magnitude of the magnetic field increases across a fast shock. Near $A = 1$, fast shocks exist when $\beta_1 \leq 1.2$ but not when $\beta_1 > 1.2$.

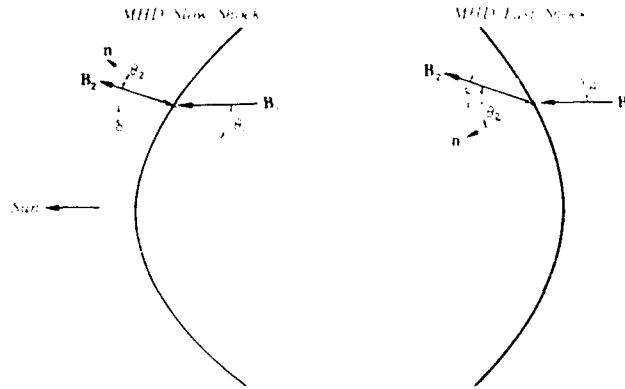


Fig. 3. The large-scale global surface of a traveling forward slow shock should have a bow-shaped surface with its nose facing the sun as shown on the left panel. The shock angle θ decreases across the slow shock by a deflection angle δ . As a forward slow shock travels outward from the sun, the decrease in the Alfvén speed causes the shock Alfvén number of a forward slow shock to reach 1 near the nose of the shock surface, and the transition from a slow shock to a fast shock begins to take place. At large heliocentric distances the slow shock is totally evolved into a fast shock. The large-scale global surface of a traveling forward fast shock has a bow-shaped surface with its nose facing away from the sun, as shown on the right panel. The shock angle increases across a fast shock.

conditions of MHD shocks can be calculated in terms of some shock parameters, which are sometimes defined in terms of physical properties on both sides of the shock. This method of solution has all shock parameters defined in terms of the upstream conditions only.

It is convenient to formulate the shock solution using an nt -s-coordinate system attached to the shock surface. Let \mathbf{n} be the unit vector normal to the shock surface and pointing in the direction of mass flow. Since the shock normal \mathbf{n} and the magnetic field vectors on both sides of a shock, \mathbf{B}_1 and \mathbf{B}_2 , are coplanar, this coplanarity plane is chosen as the nt -coordinate plane. This means that $B_s = 0$ on both sides of the shock.

We use a pair of brackets to denote the jump of a physical quantity Q across the shock, e.g.,

$$[Q] = Q_2 - Q_1$$

Let \mathbf{U} be the flow velocity in a frame of reference attached to the shock surface. At any instant the jumps in plasma and magnetic fields across an MHD shock must satisfy the following jump equations [Helfer, 1953]:

$$[B_n] = 0 \quad (1)$$

$$[\rho U_n] = 0 \quad (2)$$

$$\rho U_n [U_n] + [p] + (1/8\pi) [B_t^2] = 0 \quad (3)$$

$$4\pi \rho U_n [U_t] = B_n [B_t] \quad (4)$$

$$[U_s] = 0 \quad (5)$$

$$\rho U_n^2 [U_n^2/2 + (\gamma p/\rho)/(\gamma - 1)]$$

$$= (1/4\pi) [B_n U_t - U_n B_t] [B_t] \quad (6)$$

and

$$B_n [U_t] = [U_n B_t] \quad (7)$$

From equations (4) and (7), we can obtain

$$4\pi \rho U_n [U_n B_t] = B_n^2 [B_t] \quad (8)$$

Making use of equations (5), (7), and (8), we can write the energy equation (6) as

$$[(1 + B_t^2/B_n^2) U_n^2/2 + (\gamma p/\rho)/(\gamma - 1)] = 0 \quad (9)$$

We shall show that for given upstream conditions, from (2), (3), (8), and (9) we can obtain the exact solution of the MHD shock equations for ρ_2 , B_{t2} , p_2 , and U_{n2} as functions of three dimensionless upstream parameters: the shock Alfvén number A , the shock angle θ_1 , and B_1 . Note that these solutions are independent of the velocity components U_t and U_s . $[U_t]$ can be directly calculated from (4). The shock solution remain unchanged if an arbitrary U_s is added to both sides of the shock.

It is convenient to denote the density ratio by

$$\eta = \rho_2/\rho_1 = U_{n1}/U_{n2} \quad (10)$$

Then from (2) and (7) we obtain

$$\eta = A^2 B_{t2} / [(A^2 - 1) B_{t1} + B_{t2}] \quad (11)$$

and

$$\eta - 1 = (A^2 - 1)(B_{t2} - B_{t1}) / [(A^2 - 1) B_{t1} + B_{t2}] \quad (12)$$

In terms of A and η , we can write (3) and (9), respectively, as

$$p_2/p_1 = 1 - (B_{t2} - B_{t1}) \times [B_{t1} + B_{t2} - 2(A^2 - 1)B_n^2/B_{t2}] / 8\pi p_1 \quad (13)$$

and

$$p_2/p_1 = \eta + [(\gamma - 1)/\gamma] \{ (A^2 - 1) B_{t1} + B_{t2} \} \times [(\eta^2 - 1)(B_n^2 + B_{t1}^2) + B_{t1}^2 - B_{t2}^2] / 8\pi B_{t2} p_1 \quad (14)$$

Subtracting (13) from (14), we obtain

$$\eta - 1 + [(\gamma - 1)/\gamma] \{ (A^2 - 1) B_{t1} + B_{t2} \} \times [(\eta^2 - 1)(B_n^2 + B_{t1}^2) + B_{t1}^2 - B_{t2}^2] / 8\pi B_{t2} p_1 + (B_{t2} - B_{t1}) [B_{t1} + B_{t2} - 2(A^2 - 1)B_n^2/B_{t2}] / 8\pi p_1 = 0 \quad (15)$$

Dividing equation (15) by $\eta - 1$, making use of (12) and rearranging the result as a cubic equation in B_{t2} , we have

$$B_{t2}^3 + D_2 B_{t2}^2 + D_1 B_{t2} + D_0 = 0 \quad (16)$$

The coefficients D_i are functions of upstream conditions

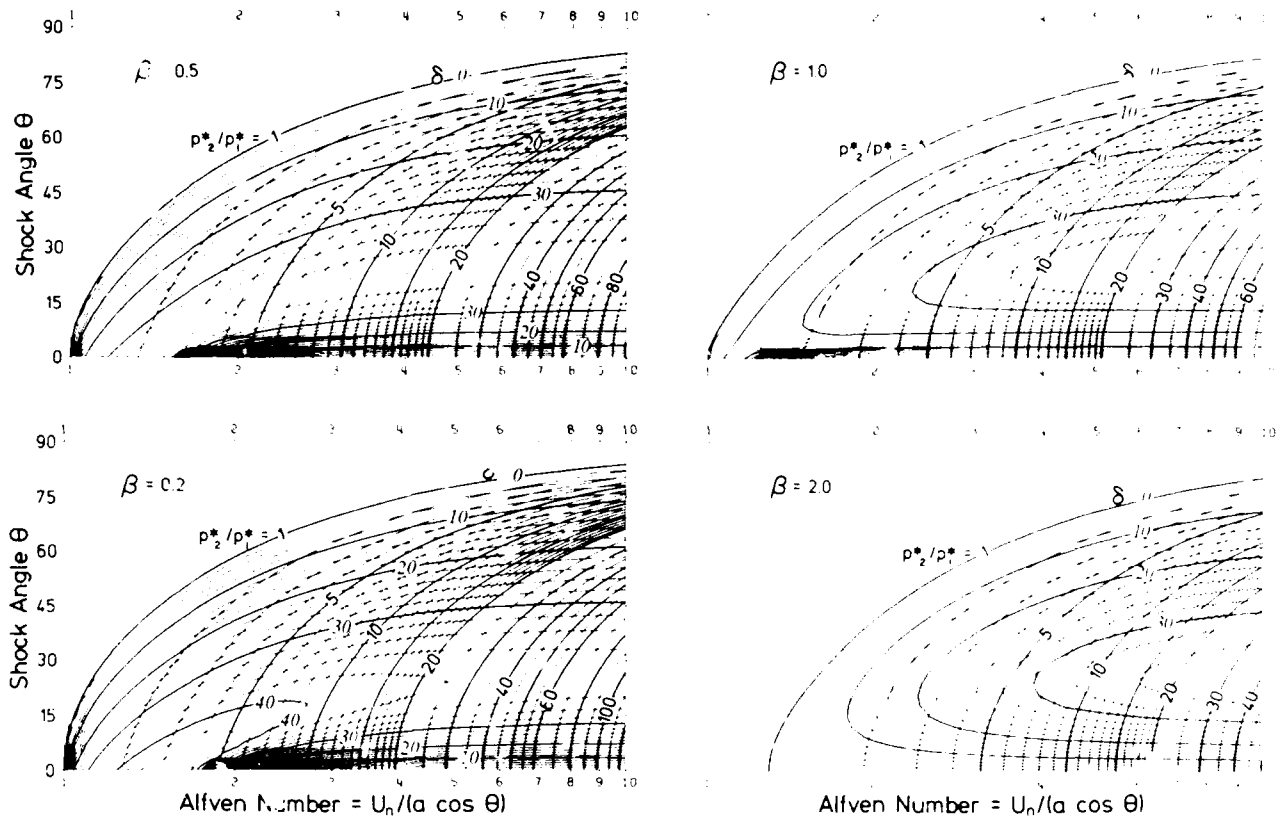


Fig. 5. For each given value of β , the jump conditions of fast shocks can be plotted as functions of A and θ_1 . When $\theta_1 = 0$, the lower limit of A equals 1 for $\beta_1 < 2/\gamma$ and equals $\gamma\beta_1/2$ for $\beta_1 > 2/\gamma$. Because the onset of transition from slow shock to fast shock can take place only when the lower limit of A is unity, it must occur in the region of interplanetary space where $\beta < 1.2$.

for slow shocks and

$$U_{n1} > C_{f1}$$

for fast shocks, where C_s and C_f are the normal speed (the phase speed) of the slow and fast magnetoacoustic wave

$$C_s^2 = (a^2 + c^2)/2 - [(a^2 + c^2)^2 - 4a^2c^2\cos^2\theta]^{1/2}/2 \quad (17)$$

and

$$C_f^2 = (a^2 + c^2)/2 + [(a^2 + c^2)^2 - 4a^2c^2\cos^2\theta]^{1/2}/2 \quad (18)$$

where c is the gasdynamic sound speed, $c^2 = \gamma p/\rho$.

From (17) we obtain that for given β_1 and θ_1 , slow shocks exist in the interval

$$\frac{1 + \gamma\beta_1/2 - [(1 + \gamma\beta_1/2)^2 - 2\gamma\beta_1\cos^2\theta_1]^{1/2}}{2\cos^2\theta_1}$$

$$< A^2 < 1$$

These limits are shown in Figure 4 for various values of β_1 . At the lower limit the deflection angle $\delta = 0$, and there is no jump in ρ , T , p , B , or p^* . At the upper limit the deflection angle δ equals θ_1 (i.e., $\theta_2 = 0$ and $B_t = 0$), and the

shocks are known as the switch-off shocks. When $\theta_1 = 0$, the lower limit equals $\gamma\beta_1/2$ for $\beta_1 < 2/\gamma$ and equals 1 for $\beta_1 > 2/\gamma$. When $\theta_1 = 90^\circ$, the lower limit equals $(1 + 2/\gamma\beta_1)^{-1}$. Note that this limiting value of A is less than 1 for all finite values of β_1 . Thus slow shocks exist for all finite values of β_1 . When $\beta_1 \gg 1$, slow shocks exist in a very small domain in the A, θ_1 parameter space, and these shocks are very weak. At the lower limit of $A^2 = (1 + 2/\gamma\beta_1)^{-1}$ when $\theta_1 = 90^\circ$, the group speed for the slow mode magnetoacoustic wave equals $(1/a^2 + 1/c^2)^{-1/2}$ which is the magnetoacoustic cusp speed.

From (18) we find that for given β_1 and θ_1 , the shock Alfvén number of fast shocks has a lower limit

$$A^2 > \frac{1 + \gamma\beta_1/2 + [(1 + \gamma\beta_1/2)^2 - 2\gamma\beta_1\cos^2\theta_1]^{1/2}}{2\cos^2\theta_1}$$

At the lower limit the fast shock approaches a fast magnetoacoustic wave, the deflection angle δ equals 0, and there is no jump in any flow property. When $\theta_1 = 0$, the lower limit equals 1 for $\beta_1 < 2/\gamma$ and equals $\gamma\beta_1/2$ for $\beta_1 > 2/\gamma$. The onset of transition from slow shock to fast shock can take place only when the lower limit of A is unity at $\theta_1 = 0$. For this reason the onset of transition must occur in the region of interplanetary space where $\beta < 2/\gamma$ or 1.2.

Let us now examine the constant contour for the deflection angle δ in Figure 5 for $\theta_1 = 0$.

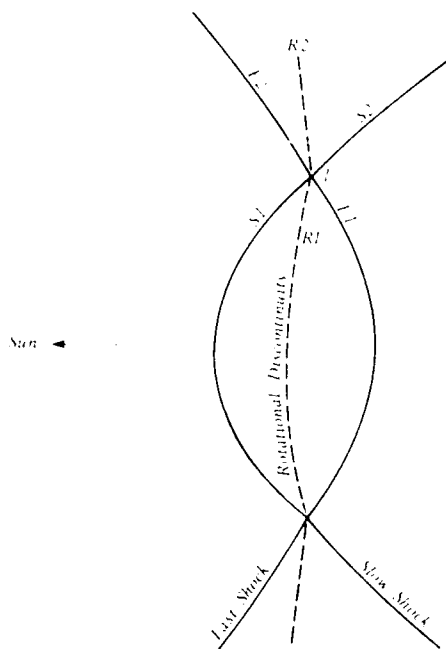


Fig. 6. The configuration of a slow-fast shock system predicted by this study for the transition of traveling forward slow shock to fast shock. The principal components of the system are a slow shock (S), a fast shock (F), and a rotational discontinuity (R), as shown in this sketch. The three surfaces of discontinuity intersect along a closed loop which may be called a transition line. The strength and the direction of each surface of discontinuity make sudden changes across the transition line.

When $\beta_1 < 2/\gamma$, the shock angle jumps from 0 to a significantly large angle for A slightly greater than 1. These solutions represent switch-on shocks. Switch-on shocks can not exist in the region where $\beta > 1.2$.

4. The Slow-Fast Shock System

During the transition the slow-fast shock system has a complicated configuration. We obtain a numerical solution to demonstrate that the principal components of such a system are a slow shock (S), a fast shock (F), and a rotational discontinuity (R), as sketched in Figure 6. The three surfaces of discontinuity intersect along a closed curve which may be called a transition line. The strength and the direction of each surface of discontinuity make sudden changes across the transition line. Let $S1$, $R1$, and $F1$ denote the discontinuities inside the closed loop of the transition line and $S2$, $R2$, and $F2$ the discontinuities outside the closed loop. At the onset of the transition process the fast shock and the rotational discontinuity are very weak discontinuities. As the system moves outward from the sun, the transition line moves laterally across the field lines in directions facing away from the noses of the three bow-shaped surfaces of discontinuity, the area enclosed by the closed loop of the transition line expands continuously, the fast shock grows stronger, and the slow shock becomes weaker.

The proposed slow-fast shock system shown in Figure 6 which may represent a physical process for the transition of slow shocks to fast shocks in the inner solar wind requires that the flow properties in the immediate neighborhood of the transition line satisfy all jump conditions of MHD discontinuity surfaces. The method of solution is to treat the normal directions of the four shock waves and the rotational angles of the two rotational discontinuities as six unknown variables. In order to analyze the flow conditions in the immediate neighborhood of the transition line it is convenient to introduce a coordinate system attached to the transition line T as shown in Figure 7. We choose the z axis tangential to the transition line and the z, x plane parallel to the magnetic field vector B upstream of the shock system. The normal directions of all surfaces of discontinuity are parallel to the x, y plane.

We present a simple numerical example in which the upstream solar wind velocity relative to the shock system U is parallel to the x, y plane. The direction of the x axis is chosen in such a way that U_x is positive upstream of the shock system. To have the shock Alfvén number for the slow shock $S2$ less than 1 and that for the fast shock $F1$ greater than 1, U_y must be positive. The example is carried out here using the following upstream conditions:

$$\beta = 0.2$$

$$U/a = 1.2$$

$$\arctan(U_y/U_x) = 30^\circ$$

$$\arctan(U_z/U_x) = 0^\circ$$

$$\arctan(B_y/B_x) = 0^\circ$$

$$\arctan(B_z/B_x) = 10^\circ$$

Let us first identify the three upstream parameters for the slow shock $S2$: β is given; the shock Alfvén number and the shock angle can be calculated once the normal direction of $S2$ is given. This means that for a given normal direction of $S2$ we can solve the cubic equation (16) for B_{t2} and calculate the magnetic field vector downstream of $S2$. Then we use (7) to calculate $[U_t]$ and the flow velocity vector downstream of $S2$. B_y and U_z downstream of $S2$ are not zero any more. The next step is to calculate p_2 and ρ_2 using (11) and (13). Therefore, once the normal direction of $S2$ is given, we can determine all flow conditions downstream of $S2$ by solving a system of nonlinear algebraic equations. Following the same procedure, once the normal direction of $F1$ is given, we can determine all flow conditions downstream of $F1$.

Since the shock Alfvén number of $R1$ and $R2$ must be unity, this condition is used to determine the normal direction of the two rotational discontinuities. The strength of a rotational discontinuity may be measured by the rotational angle of the tangential magnetic field vector. We use the right-hand rule to determine the positive direction for the rotational angle. Now we can calculate all flow conditions downstream of $R1$ and $R2$, respectively, for given

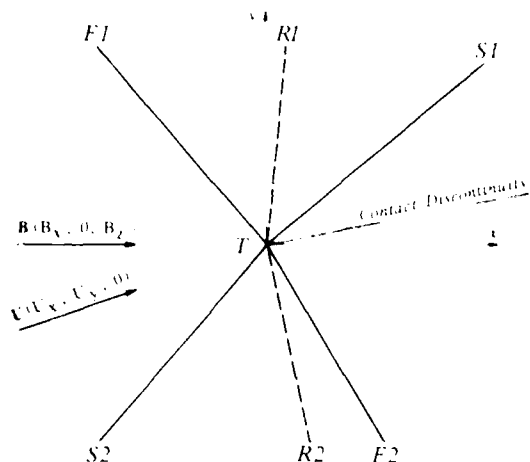


Fig. 7. A coordinate system attached to the transition line T is used for the analysis of the flow conditions in the immediate neighborhood of T. The z axis is tangential to the transition line and the x,y plane is parallel to the magnetic field vector \mathbf{B} upstream of the shock system. We study a simple case in which the upstream solar wind velocity relative to the shock system \mathbf{U} is parallel to the x,y plane. The direction of the x axis is chosen in such a way that U_x is positive upstream of the shock system. S1, R1, and F1 denote the discontinuities inside the closed loop of the transition line. S2, R2, and F2 are outside the closed loop. The flow downstream of S1 and F2 is separated by a contact discontinuity.

rotational angles. At this point, we have calculated the flow properties U/a , B , p , and β downstream of R1 and R2.

Once the normal directions of F2 and S1 are given, we can calculate the three upstream shock parameters (A , β , and θ) for each shock. Once again, we can solve the nonlinear algebraic

system (equations (16), (7), (11), and (13)) to determine the flow conditions downstream of the two shocks. In summary, the flow conditions downstream of S1 and F2 are functions of six parameters: the normal directions of the four shock waves and the rotational angles of the two rotational discontinuities. The six parameters are treated as six unknown variables to be determined by boundary conditions for the flows downstream of S1 and F2.

The flows downstream of S1 and F2 are separated by a contact discontinuity. Across the contact surface the flow must satisfy three conditions: (1) the magnetic field \mathbf{B} be continuous, (2) the thermal pressure p be continuous, and (3) the velocity vectors be parallel. The three conditions are actually represented by six scalar equations. We can numerically solve the system of nonlinear equations for the six unknown variables. Note that since $\mathbf{U} \times \mathbf{B}$ is continuous across each of the MHD shocks and rotational discontinuities, conditions 1 and 3 guarantee that \mathbf{U} is also continuous across the contact discontinuity. Following the procedure outlined above, we have obtained a numerical solution which satisfies the jump conditions across the four shock waves, two rotational discontinuities, and one contact discontinuity. Important parameters of the solution identified with each shock and rotational discontinuity obtained from this example are listed in Table 1.

If $B_z = 0$ upstream of the slow-fast shock system, $B_z = 0$ everywhere in the immediate neighborhood of T. The rotational angles are zero for both R1 and R2. The problem is reduced to solving a nonlinear system for four unknown directional angles of the shocks.

The analysis of the flow conditions in the immediate neighborhood of the transition line suggests that during the transition process the large-scale slow-fast shock system can have a configuration as shown in Figure 6. This model

TABLE 1. An Illustrative Example for the Slow-Fast Shock System

Discontinuity	S1	S2	F1	F2	R1	R2
Normal Direction of Each Discontinuity						
$\arctan(n_y/n_x)$	-48.8	-44.0	34.6	37.2	9.7	-6.0
Direction of U and B Behind Each Discontinuity						
$\arctan(U_y/U_x)$	21.2	32.3	18.2	21.2	18.3	31.6
$\arctan(U_z/U_x)$	4.3	1.1	3.4	4.3	3.4	1.5
$\arctan(B_y/B_x)$	-13.2	-1.7	-11.4	-13.2	-11.4	-2.9
$\arctan(B_z/B_x)$	12.4	9.7	12.8	12.4	12.9	10.2
Rotation Angle of B_t					-0.02	7.06
Jump Conditions of the Four Shocks						
β_1	0.200	0.200	0.200	0.322		
A_1	0.474	0.467	1.476	1.663		
θ_1	39.15	44.89	35.84	41.19		
B_2/B_1	0.976	0.972	1.196	1.207		
ρ_2/ρ_1	1.296	1.283	1.221	1.239		
T_2/T_1	1.195	1.186	1.173	1.174		
p_2/p_1	1.548	1.521	1.432	1.455		
β_2	0.325	0.322	0.200	0.322		
A_2	0.416	0.412	1.336	1.493		
θ_2	37.36	43.19	47.34	51.44		

for the transition process infers that a traveling forward slow shock observed in the inner solar wind can be part of a single bow-shaped slow shock surface or of a complicated slow-fast shock system. It also infers that the transition process provides a mechanism which generates rotational discontinuities in interplanetary space. The presence of shock-rotational discontinuity sequences in the observational data (C. F. Kennel, private communication, 1986) possibly supports the existence of slow-fast shock systems predicted by this model.

Acknowledgments. The author thanks A. J. Hundhausen, T. E. Holzer, and B. C. Low for providing him with a preprint of their manuscript on slow shocks preceding some coronal mass ejections. This work was supported by the Air Force Office of Scientific Research under contract 86-610.

The Editor thanks B. Roberts and H. E. Strauss for their assistance in evaluating this paper.

References

- Bazer, J., and W. B. Ericson, Hydromagnetic shocks, *Astrophys. J.*, **129**, 758, 1959.
- Burlaga, L. F., and J. K. Chao, Reverse and forward slow shocks in the solar wind, *J. Geophys. Res.*, **76**, 7516, 1971.
- Chao, J. K., and S. Olbert, Observation of slow shocks in interplanetary space, *J. Geophys. Res.*, **75**, 6394, 1970.
- Dryei, M., Interplanetary shock waves: Recent developments, *Space Sci. Rev.*, **17**, 277, 1975.
- Edmiston, J. P., and C. F. Kennel, A parametric study of slow shock Rankine-Hugoniot solutions and critical Mach numbers, *J. Geophys. Res.*, **91**, 1361, 1986.
- Feldman, W. C., D. N. Baker, S. J. Bame, J. Birn, J. T. Gosling, E. W. Hones, Jr., and S. J. Schwartz, Slow mode shocks: A semipermanent feature of the distant geomagnetic tail, *J. Geophys. Res.*, **90**, 233, 1985.
- Hada, T., and C. F. Kennel, Nonlinear evolution of slow waves in the solar wind, *J. Geophys. Res.*, **90**, 531, 1985.
- Helper, H. L., Magnetohydrodynamic shock waves, *Astrophys. J.*, **117**, 177, 1953.
- Hildner, E., Mass ejections from the solar corona into interplanetary space, in *Study of Traveling Interplanetary Phenomena 1977*, edited by M. A. Shea, D. F. Smart, and S. T. Wu, pp. 3-21, D. Reidel, Hingham, Mass., 1977.
- Kulikovskii, A. G., and G. A. Lyubimov, *Magnetohydrodynamics*, p. 96, State Physics and Mathematics Press, Moscow, 1962.
- Lust, R., Stationäre magneto-hydrodynamische stosswellen beliebiger starke, *Z. Naturforsch.*, **10a**, 125, 1955.
- Lynn, Y. M., Magnetohydrodynamic shocks in nonaligned flow, *Phys. Fluids*, **9**, 314, 1966.
- MacQueen, R. M., Coronal transients: A summary, *Philos. Trans. R. Soc. London, Ser. A*, **297**, 605, 1980.
- Neubauer, F. M., Nonlinear interaction of discontinuities in the solar wind and the origin of slow shocks, *J. Geophys. Res.*, **81**, 2248, 1976.
- Richter, A. K., H. Rosenbauer, F. M. Neubauer, and N. G. Ptitsyna, Solar wind observations associated with a slow-forward shock wave at 0.31 AU, *J. Geophys. Res.*, **90**, 7581, 1985.
- Rosenau, P., and Suess, S. T., Slow shocks in interplanetary medium, *J. Geophys. Res.*, **82**, 3643, 1977.
- Sears, W. R., and E. L. Resler, Jr., Sub- and super-Alfvénic flows past bodies, *Adv. Aerosp. Sci.*, **3-4**, 637, 1961.
- Sheeley, N. R. Jr., R. A. Howard, M. J. Koomen, D. J. Michels, R. Schwenn, K. H. Muhlhauser, and H. Rosenbauer, Coronal mass ejections and interplanetary shocks, *J. Geophys. Res.*, **90**, 163, 1985.
- Whang, Y. C., Slow shocks around the sun, *Geophys. Res. Lett.*, **9**, 1081-1084, 1982.
- Whang, Y. C., Transition of traveling interplanetary slow shock to fast shock, *Eos Trans. AGU*, **67**, 327, 1986a.
- Whang, Y. C., Solar wind flow upstream of the coronal slow shock, *Astrophys. J.*, **307**, 838, 1986b.

Y. C. Whang, Department of Mechanical Engineering, Catholic University, Washington, DC 20064.

(Received August 28, 1986;
revised December 23, 1986;
accepted January 9, 1987.)

EVOLUTION OF INTERPLANETARY SLOW SHOCKS

Y. C. Whang

Department of Mechanical Engineering, Catholic University of America, Washington, D. C.

Abstract. The possible existence of traveling forward slow shocks, their global geometry and their transition to forward fast shocks have been discussed in a recent paper. The decrease in the Alfvén speed at increasing heliocentric distance causes the evolution of a forward slow shock into a forward fast shock. During the transition the shock system consists of a slow shock, a fast shock, and a rotational discontinuity. This paper continues to discuss three aspects about the evolution of interplanetary slow shocks. We first present a survey of slow shock solutions in a three-dimensional A, θ, β parameter space. Here $A = U_n / (a \cos \theta)$ is the shock Alfvén number, U_n the normal component of the relative shock speed, a the Alfvén speed, θ the acute angle between the shock normal and the magnetic field, and β the ratio of the thermal pressure p to the magnetic pressure $B^2/8\pi$. In a region where the plasma β value is on the order of 1 or greater, the jumps in thermodynamic properties across a slow shock are small but the directional changes for the magnetic field and the relative flow velocity are not necessarily small. On the other hand, in the region where the plasma β value is on the order of 0.1 or less, the jumps of all physical properties across a slow shock may vary over a wide range of magnitudes. Next, we discuss that at the onset of the transition process an interplanetary slow shock smoothly converts to a system consisting of a slow shock, a very weak rotational discontinuity (an Alfvén wave), and a very weak fast shock (a fast MHD wave). We also show that during the transition, the amplitude of fluctuations in flow velocity and magnetic fields are large in the turbulent region behind the fast shock.

1. Introduction

Traveling interplanetary shocks are associated with coronal mass ejections and flares. When the speed of the ejected material relative to the ambient solar wind exceeds the local magnetoacoustic speed, a magnetohydrodynamic (MHD) shock front forms at the leading edge of the compressed ambient plasma shell. The solutions of MHD shocks may be expressed as functions of three dimensionless upstream conditions: the shock Alfvén number based on the relative shock speed $A = U_n / (a \cos \theta)$, the shock angle θ , and the plasma β value. Here U_n is the normal component of the relative shock speed, a the Alfvén speed, θ the acute angle between the shock normal and the magnetic field, and β the ratio of the thermal pressure p to the magnetic pressure $B^2/8\pi$. Two kinds of MHD shocks, the fast and the slow shocks, may exist. A shock is a slow shock if the shock Alfvén number A is less than 1 and is a fast shock if A is greater than 1. The

plasma density, the thermal pressure, and the total pressure (the sum of the thermal and the magnetic pressures) all increase across an MHD shock. The magnetic field and the shock angle decrease across a slow shock and increase across a fast shock. Observations of slow shocks have been reported by Chao and Olbert [1970], Burlaga and Chao [1971], Richter et al. [1985], and Feldman et al. [1985].

In a recent paper [Whang, 1987] (hereafter referred to as paper 1), we studied traveling interplanetary forward slow shocks and their transition to forward fast shocks in the inner solar wind. In coronal space, the Alfvén speed is of the order of 1000 km/s; the shock Alfvén number of an MHD shock in the inner solar wind can be less than 1 and the shock can be a slow shock. An important characteristic of slow shocks (and slow MHD waves) is that they are upstream-inclined [Sears and Resler, 1961]. The large-scale global surface of a forward slow shock should have a bow-shaped surface with its nose facing the Sun. Recently, Hundhausen et al. [1987] studied the outward motion for coronal mass ejections observed by the Skylab coronagraph and the SMM coronagraph. Their conclusion supports the possible formation of forward slow MHD shocks immediately in front of some coronal mass ejections. They pointed out that in a diverging radial background field a large-scale traveling forward slow shock may have a rather flat configuration, because the upstream inclined nature of forward slow MHD shocks is relative to the magnetic field geometry. Thus, the observed flattening of the tops of some mass ejection loops support the possible existence of traveling forward slow shocks.

The Alfvén speed decreases at increasing heliocentric distance in the inner solar wind. The variation of the shock speed relative to the solar wind flow is not well understood. Presume that the Alfvén speed decreases at a rate faster than the relative shock speed if the relative shock speed also decreases at increasing heliocentric distance. Then as a forward slow shock travels outwards from the Sun, the decrease in the Alfvén speed causes the shock Alfvén number of a forward slow shock to become greater than 1 at increasing heliocentric distances and the shock evolves from a forward slow shock into a forward fast shock. Because the fast-mode MHD waves and MHD shocks are downstream-inclined, the large-scale global surface of a traveling forward fast shock has a bow-shaped surface with its nose facing away from the Sun.

Paper 1 suggested a possible process for the transition of a forward slow shock to a forward fast shock. During the transition, the system consists of a forward slow shock, a forward fast shock, and a forward rotational discontinuity. The three surfaces of discontinuity intersect along a closed transition line. At the onset of the transition process the fast shock and the rotational discontinuity are very weak. As the

Copyright 1988 by the American Geophysical Union.

Paper number 7A9249.

0148-0227/88/007A-9249\$02.00

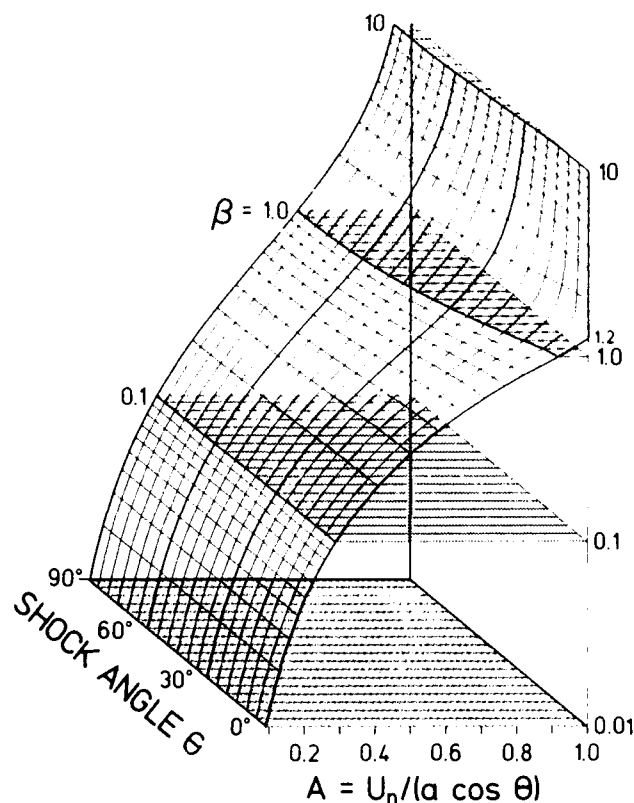


Fig. 1. This figure depicts the domain in which slow shock solutions exist in the three-dimensional parameter space. The domain of slow shock solutions in the A, θ, β_1 parameter space shrinks as the plasma β_1 value increases. The major change takes place when β_1 is between 0.1 and 1. The change becomes very small at very large or very small β_1 .

system moves outward from the Sun the transition line moves laterally across the field lines, the area enclosed by the closed loop of the transition line expands continuously, the fast shock grows stronger, and the slow shock becomes weaker. Eventually, the forward slow shock diminishes and the entire system evolves into a forward fast shock. This proposed transition process satisfies the necessary condition that the flows in the immediate neighborhood of the transition line meet all MHD jump conditions. On November 12, 1978, ISEE 1 and 3 observed a high-speed, quasi-parallel, interplanetary forward fast shock which was followed by a rotational discontinuity [Kennel et al., 1984a, b]. This event resembles the kind of transition process described here.

In this paper, we will discuss three aspects of traveling interplanetary forward slow shocks. We will first present a survey of slow shocks in a three dimensional parameter space. Then, we will discuss the onset of the transition process. Finally, we will discuss the turbulent nature of the flow field behind the fast shock during the transition process.

2. A Three-Dimensional Parametric Survey of Slow Shocks

In paper 1, we obtained a direct and simple solution for the jump conditions of MHD oblique shocks. The method calculates the exact solution

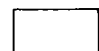
of the MHD shock equations as functions of three dimensionless upstream parameters: the shock Alfvén number A , the shock angle θ_1 , and β_1 . The subscript 1 denotes the flow condition on the front side (upstream) of a shock, and 2 denotes the flow condition on the back side (downstream). The plasma density ρ , the thermal pressure p , and the total pressure p^* (the sum of the thermal and the magnetic pressures) all increase across an MHD shock. The magnetic field and the shock angle decrease across a slow shock. The decrease in shock angles across a slow shock may be called the deflection angle δ . In this section, we present the solution of slow shocks in a three-dimensional parameter space, the A, θ, β -space as shown in Figures 1-3. All calculations are carried out using the ratio of specific heats $\gamma = 5/3$ for fully ionized plasma. A parametric study of MHD slow shocks in different combination of two dimensional parameter space has also been reported by Edmiston and Kennel [1986].

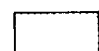
Let us first examine the domain in which slow shock solutions exist in the three dimensional parameter space (Figure 1). Slow shocks exist at all shock angles (from 0° to 90°) and at all β values in a certain interval of the shock Alfvén number A ,

$$\frac{1 + \gamma\beta_1/2 - \{(1 + \gamma\beta_1/2)^2 - 2\gamma\beta_1\cos^2\theta_1\}^{1/2}}{2\cos^2\theta_1} < A^2 < 1$$

DENSITY RATIO

 < 1.5

 $1.5-2.5$

 > 2.5

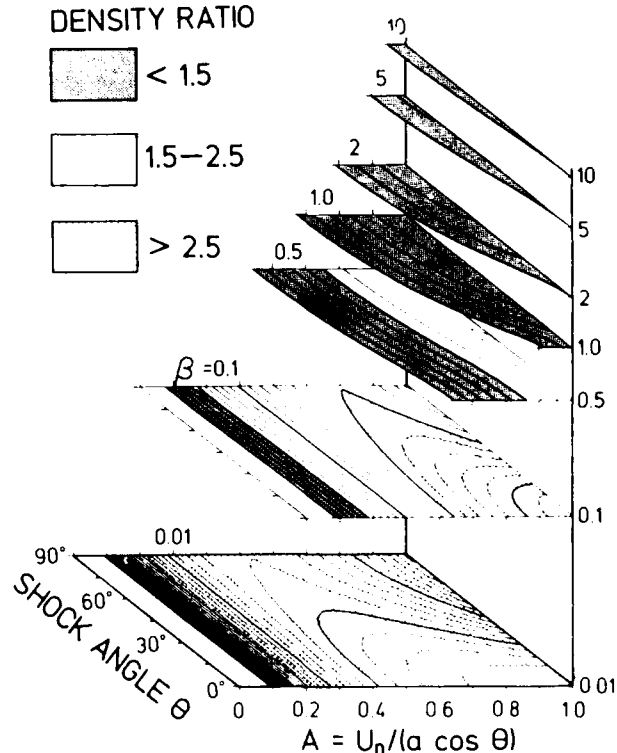


Fig. 2. This figure presents a three-dimensional plot of the constant contours of the density ratios across MHD slow shocks. The jump in density across a slow shock, ρ_2/ρ_1 , varies over a wide range of magnitude, from very weak to moderately strong, in the low β region (where $\beta_1 < 0.1$). On the other hand, only weak discontinuity in density across a slow shock ($\rho_2/\rho_1 < 1.5$) occurs in the high β region (where $\beta_1 > 1.0$).

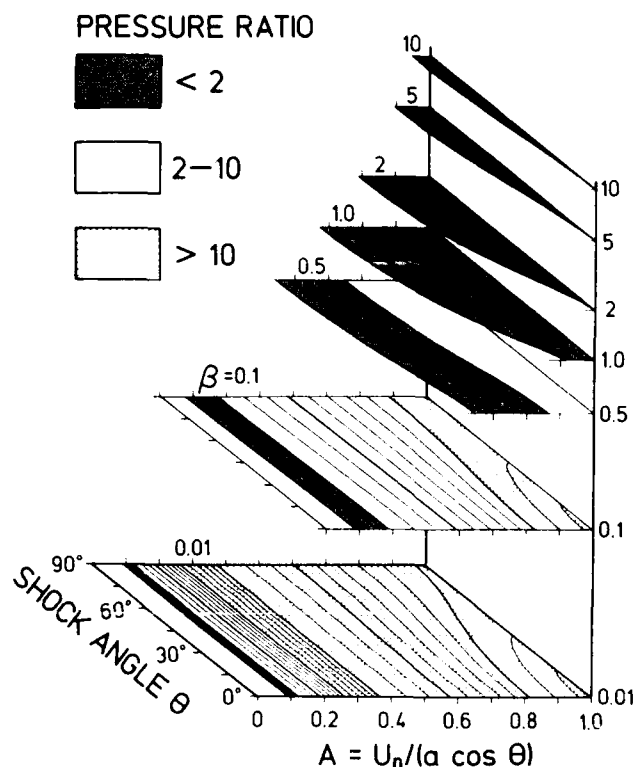


Fig. 3. This figure presents a three-dimensional plot of the constant contours for the pressure ratios across MHD slow shocks, p_2/p_1 . We can reach the same conclusion regarding the discontinuity in pressure as functions of the plasma β value from Figures 2 and 3. In the coronal space where the β value of the solar wind is much less than 1, the change in thermodynamic properties across a slow shock may vary over a wide range. On the other hand, near 1 AU where the average β value of the solar wind is in the order of 1, the jump in thermodynamic properties across a slow shock is always very weak.

The lower limit is equivalent to the evolutionary condition that

$$U_{n1} > C_{s1}$$

where C_s is the normal speed (the phase speed) of the slow magnetoacoustic wave. At the lower limit the deflection angle $\delta = 0$, and there is no jump in ρ , T , p , B , or p^* . When $\theta_1 = 90^\circ$, the lower limit equals $(1 + 2/\gamma\beta_1)^{-1}$. When $\theta_1 = 0$, the lower limit equals $\gamma\beta_1/2$ for $\beta_1 < 2/\gamma$ and equals 1 for $\beta_1 > 2/\gamma$. The slow shocks at the upper limit of $A = 1$ are the switch-off shocks which turn off the tangential component of the magnetic field (i.e., $\theta_2 = 0$ and $\delta = \theta_1$). The domain of slow shock solutions in the A, θ_1 parameter space shrinks as the plasma β_1 value increases as shown in Figure 1. The major change takes place when β_1 is between 0.1 and 1. The change becomes very small at very large or very small β_1 .

Figures 2 and 3, respectively, present the constant contours for the jumps in density and pressure across slow shocks, namely the ratio ρ_2/ρ_1 or p_2/p_1 , as functions of three independent parameters, A , θ_1 and β_1 . If we call those slow shocks with $\rho_2/\rho_1 < 1.5$ as weak discontinuities in density and those with $\rho_2/\rho_1 > 2.5$ as strong

discontinuities in density, then from Figure 2 we can reach a conclusion that slow shocks covering a wide range of strength for the discontinuity in density (from very weak to moderately strong) exist in the low β region (where $\beta_1 \leq 0.1$). On the other hand, only weak discontinuities in density exist in the high β region (where $\beta_1 \geq 1$). Next, we study the discontinuities in pressure for slow shocks. From a plot of the pressure ratios in Figure 3 we can reach the same conclusion. In the coronal space where the β value of the solar wind is much less than 1, the jump in thermodynamic properties across a slow shock may vary over a wide range. On the other hand, near 1 AU where the average β value of the solar wind is on the order of 1, the jump in thermodynamic properties across a slow shock is always very weak.

The jumps in other physical properties offer different ways to measure the effect of an MHD slow shock on the plasma and fields. The constant contours for B_2/B_1 at $\beta = 0.2$ were plotted in Figure 1 of paper 1. A whole range of changes in B_2/B_1 , from 0 to 1, may take place in the domain of slow shock solutions at $\beta = 0.2$. Across an MHD shock the magnetic field vector abruptly changes its direction by the deflection angle. The relative flow velocity also make a sudden change in its direction across an MHD shock by an angle approximately in the similar magnitude as the deflection angle. Constant contours for the deflection angle, $0 \leq \delta \leq 90^\circ$, were plotted in Figure 4 of paper 1. All field-related properties, such as B_2/B_1 and δ , change over the same ranges in the domain of slow shock solutions for any given value of β_1 .

The plasma β value is on the order of 0.1 in coronal space, it increases at increasing heliocentric distance. In the region where the plasma β value is on the order of 0.1 or less, all physical properties may jump across a slow shock over a wide range magnitudes. Near 1 AU where the plasma β value is on the order of 1 or greater, the jumps in thermodynamic properties across a slow shock must be small but the jumps in field-related properties are not necessarily small. Traditionally, we measure the strength of a shock by the jump in density or pressure across the shock (ρ_2/ρ_1 or p_2/p_1). Actually, a shock may be called a weak shock wave only when the discontinuity in every quantity is small. A slow shock with small discontinuity in thermodynamic properties is not necessarily a weak one. When the discontinuities in thermodynamic properties are small, the identification of a slow shock becomes difficult from plasma observations.

3. Onset of the Transition Process

It is convenient to discuss the onset of the transition process using an AB coordinate system as shown in Figure 4. Here A is the shock Alfvén number and B stands for the ratio of the magnetic field B_2/B_1 . We may call the region in which both A and B_2/B_1 are greater than 0 and less than 1 a slow region, the quadrant in which both A and B_2/B_1 are greater than 1 the fast quadrant, and the point at which both A and B_2/B_1 are unity the Alfvén point. The domain of solutions for slow shocks is limited to the slow region in the AB plane. As discussed in the previous section, the domain shrinks as the plasma β_1 value increases. The domain of solutions for the fast shocks is

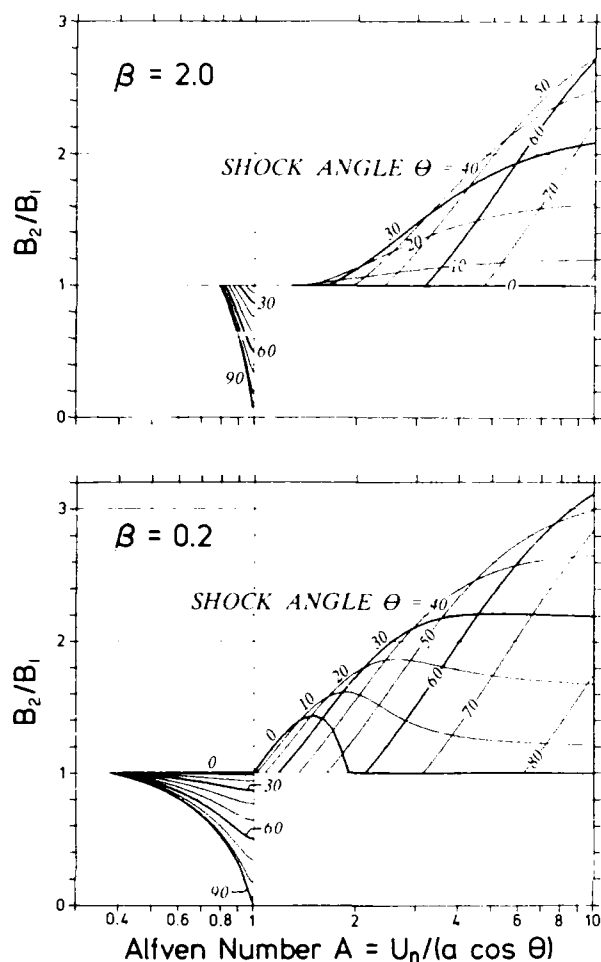


Fig. 4. The upper panel plots the solution curves for MHD shocks with $\beta \geq 2/\gamma$ and the lower panel plots the solution curves with $\beta \leq 2/\gamma$. At the onset of the transition process the interplanetary slow shock near the nose smoothly converts to a system consisting of a slow shock, a very weak rotational discontinuity (an Alfvén wave), and a very weak fast shock (a fast MHD wave). When $\beta \geq 2/\gamma$, fast shock solutions do not exist near the Alfvén point where both A and B_2/B_1 are unity. Thus, the onset of transition must occur in the region of interplanetary space where $\beta < 2/\gamma$ or 1.2. At the onset of transition the slow shock, the weak rotational discontinuity and the weak fast shock move at the same speed equal to a in the solar wind frame of reference.

limited to the fast quadrant of the AB plane. Rotational discontinuities and Alfvén waves are represented by a single point, the Alfvén point of the AB plane.

A forward slow shock can travel in the inner solar wind having a bow-shaped surface with its nose facing the Sun. A large pressure jump bounded by the discontinuity surface of the forward slow shock propagates forward in the solar wind frame of reference. On the curved surface of the forward slow shock the shock Alfvén number is less than 1 everywhere, although it varies from point to point. The slow shock should be relatively stronger at the nose. It becomes weaker on the flank and asymptotically approaches slow mode MHD waves. Across all points of this single surface the shock solutions are located on the slow region of the AB plane.

As the forward slow shock travels outwards from the Sun, the decrease in the Alfvén speed causes the shock Alfvén number to reach 1 near the nose of the shock surface, the transition from a forward slow shock to a forward fast shock begins to take place. At the onset of the transition process the interplanetary forward slow shock smoothly converts to a system consisting of a forward slow shock, a very weak forward rotational discontinuity (an Alfvén wave), and a very weak forward fast shock (a fast MHD wave). On the AB plane the mapping of the slow shock solutions near the nose lies in the immediate neighborhood of the Alfvén point in the slow region. As shown in the lower panel of Figure 4 the shock angle approaches 0° . The limiting case of the shock is a gasdynamic normal shock with finite strength. The slow shock continues to carry the finite jumps in pressure and density and propagates in the solar wind frame. The rotational discontinuity maps with the Alfvén point. On the AB plane, the newly generated weak fast shock maps with points in the immediate neighborhood of the Alfvén point in the fast quadrant.

A smooth conversion requires that at the onset of transition the three discontinuity surfaces (the slow shock, the weak rotational discontinuity and the weak fast shock) move at the same speed. In Figure 4, the upper panel plots the solution curves for MHD shocks on the AB plane with $\beta > 2/\gamma$ and the lower panel plots the solution curves with $\beta < 2/\gamma$. When $\beta > 2/\gamma$, fast shock solutions do not exist near the Alfvén point in the AB plane. Thus, a smooth conversion at the onset of transition is not possible when $\beta > 2/\gamma$ or 1.2. The onset of transition must occur in the region of interplanetary space where $\beta < 2/\gamma$ or 1.2.

4. Turbulent Flow behind the Fast Shock

Figure 5 shows the constant contours of deflection angle and the pressure ratio in the domain of fast shock solutions in the $A\theta$ plane at a given β value. The shock Alfvén number of fast shocks has a lower limit

$$A^2 > \frac{1 + \gamma\beta_1/2 + \{(1 + \gamma\beta_1/2)^2 - 2\gamma\beta_1\cos^2\theta_1\}^{1/2}}{2\cos^2\theta_1}$$

At the lower limit the fast shock approaches a fast magnetoacoustic wave, the deflection angle θ equals 0, and there is no jump in any physical property.

When a forward transition system consisting of a slow shock, a fast shock, and a rotational discontinuity propagates in interplanetary space with $\beta < 1.2$, the shock Alfvén numbers of the fast shock near the nose are slightly greater than 1 and the shock angles are very small. From Figure 5 we can see that the deflection angles are quite significant and change rapidly for fast shocks in this neighborhood of the parameter space. The shocks significantly change the directions of the magnetic field and the relative flow velocity. The fast shocks in this neighborhood of the parameter space are near switch-on shocks. Switch-on shocks and near switch-on shocks may exist in the region where $\beta < 1.2$. Small random fluctuations in plasma flow and magnetic fields on the front side of the

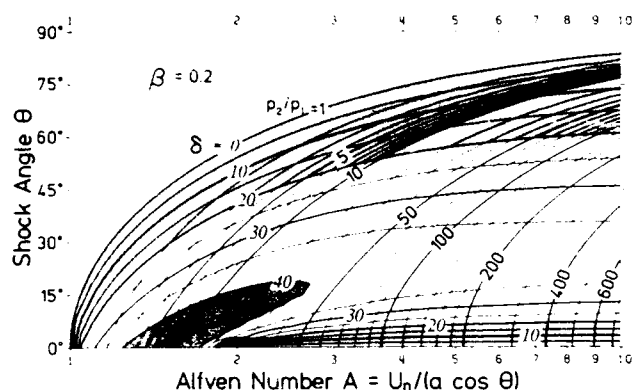


Fig. 5. When a transition system propagates in interplanetary space with $\beta < 1.2$, the shock Alfven numbers of the fast shock near the nose are slightly greater than 1 and the shock angles are very small. In this neighborhood of the parameter space, the fast shocks significantly change the directions of the magnetic field and the relative flow velocity. Small random fluctuations in plasma flow and magnetic fields on the front side of the shock are considerably amplified. The flow becomes very turbulent and the amplitude of fluctuations in flow velocity and magnetic fields are large in the turbulent region behind the fast shock.

shock are considerably amplified across the near switch-on shocks. The flow becomes very turbulent behind the shocks. Therefore, during the transition, the amplitude of fluctuations in flow velocity and magnetic fields are large in the turbulent region behind the fast shock. When ISEE-1 and -3 observed a possible forward transition system consisting of a forward fast shock ahead of a rotational discontinuity on November 12, 1978, an intense MHD turbulence was also observed in the region between the two discontinuity surfaces [Kennel et al., 1984b].

5. Summary

In this paper, we discuss three aspects of traveling interplanetary forward slow shocks: (1) A survey of slow shocks in a three-dimensional parameter space, (2) the onset of the transition process, and (3) the turbulent nature of the flow field behind the fast shock during the transition process.

The parametric study shows that in the region where the plasma β value is of the order of 0.1 or less, the jumps of all physical properties across a slow shock may vary over a wide range of magnitudes. On the other hand, in a region where the plasma β value is on the order of 1 or greater, the jumps in thermodynamic properties across a slow shock are small but the jumps in field-related properties are not necessarily small.

Next, we use a graphical demonstration to explain that the onset of the transition process can occur in the region of interplanetary space where $\beta < 2/\gamma$ or 1.2. At the onset of the transition process the interplanetary slow shock near the nose of the slow shock smoothly converts to a system consisting of a slow shock, a very weak rotational discontinuity (an Alfven wave), and a very weak fast shock (a fast MHD wave). The

three surfaces of discontinuity move at nearly the same speed (the Alfven speed) in the solar wind frame of reference.

Finally, we show that during the transition, the amplitude of fluctuations in flow velocity and magnetic fields are large in the turbulent region behind the fast shock.

Acknowledgments. The author thanks A. J. Hundhausen, T. E. Holzer, and B. C. Low for providing him with a preprint of their manuscript on slow shocks preceding some coronal mass ejections. This work was supported by the Air Force Office of Scientific Research under contract 86-160.

The Editor thanks S. T. Suess and two other referees for their assistance in evaluating this paper.

References

- Burlaga, L. F., and J. K. Chao, Reverse and forward slow shocks in the solar wind, *J. Geophys. Res.*, **76**, 7516, 1971.
- Chao, J. K., and S. Olbert, Observation of slow shocks in interplanetary space, *J. Geophys. Res.*, **75**, 6394, 1970.
- Edmiston, J. P., and C. F. Kennel, A parametric study of slow shock Rankine-Hugoniot solutions and critical Mach numbers, *J. Geophys. Res.*, **91**, 1361, 1986.
- Feldman, W. C., D. N. Baker, S. J. Bame, J. Birn, J. T. Gosling, E. W. Hones, Jr., and S. J. Schwartz, Slow mode shocks: A semipermanent feature of the distant geomagnetic tail, *J. Geophys. Res.*, **90**, 233, 1985.
- Hundhausen, A. J., T. E. Holzer, and B. C. Low, Do slow shocks precede some coronal mass ejections?, *J. Geophys. Res.*, **92**, 11,173, 1987.
- Kennel, C. F., F. L. Scarf, F. V. Coroniti, C. T. Russell, K. P. Wenzel, T. R. Sanderson, P. Van Nes, W. C. Feldman, G. K. Parks, E. J. Smith, B. T. Tsurutani, F. S. Mozer, M. Temerin, R. R. Anderson, J. D. Scudder, and M. Scholer, Plasma and energetic particle structure upstream of a quasi-parallel interplanetary shock, *J. Geophys. Res.*, **89**, 5419, 1984a.
- Kennel, C. F., J. P. Edmiston, F. L. Scarf, F. V. Coroniti, C. T. Russell, E. J. Smith, B. T. Tsurutani, J. D. Scudder, W. C. Feldman, Structure of the November 12, 1978, quasi-parallel interplanetary shock, *J. Geophys. Res.*, **89**, 5436, 1984b.
- Richter, A. K., H. Rosenbauer, F. M. Neubauer, and N. G. Ptitsyna, Solar wind observations associated with a slow-forward shock wave at 0.31 AU, *J. Geophys. Res.*, **90**, 7581, 1985.
- Sears, W. R., and E. L. Resler, Jr., Sub- and super-Alfvenic flows past bodies, *Adv. Acrosp. Sci.*, **3-4**, 637, 1961.
- Whang, Y. C., Slow shocks and their transition to fast shocks in the inner solar wind, *J. Geophys. Res.*, **92**, 4349, 1987.

Y. C. Whang, Department of Mechanical Engineering, Catholic University of America, Washington, DC 20064.

(Received August 5, 1987;
revised November 17, 1987;
accepted November 17, 1987.)

FORWARD-REVERSE SHOCK PAIRS ASSOCIATED WITH CORONAL MASS EJECTIONS

Y. C. Whang

Department of Mechanical Engineering, Catholic University of America, Washington, D. C.

Abstract. For some coronal mass ejections (CMEs), their interaction with the ambient solar wind can produce a forward-reverse shock pair. The high-speed mass ejecta compresses the plasma near the top of the CME on both sides of the tangential discontinuity which separates the CME plasma from the ambient solar wind plasma. The front of the compressed CME plasma propagates in the reverse direction relative to the ejecta flow, it may steepen to form a reverse slow shock. The front of the compressed solar wind plasma also propagates in the forward direction relative to the ambient solar wind and it may steepen to form a forward shock. The forward-reverse shock pair associated with CMEs moves outward in interplanetary space and evolves into a pair of fast shocks. The interplanetary manifestation of some CMEs is pictured as a magnetic cloud accompanied by a shock pair: a forward shock precedes the cloud and a reverse shock either within or behind the cloud.

1. Introduction

The possible existence of forward slow shocks preceding some coronal mass ejections (CMEs) has been suggested by Whang [1987] and by Hundhausen et al. [1987]. Whang also showed that transition from a traveling forward slow shock to a forward fast shock can take place in interplanetary space. This paper suggests that a reverse slow shock associated with CMEs can form under some circumstances, and it shows that when such a shock is present it will evolve into reverse fast shock.

The solutions of magnetohydrodynamic (MHD) shocks may be expressed as functions of three dimensionless upstream parameters: the shock Alfvén number based on the relative shock speed $A = U_n/(a \cos \theta)$, the shock angle θ , and the plasma β value. Here U_n is the normal component of the relative shock speed, a the Alfvén speed, θ the acute angle between the shock normal and the magnetic field, and β the ratio of the thermal pressure p to the magnetic pressure $B^2/8\pi$. Two kinds of MHD shocks, the fast and the slow shocks, may exist. A shock is a slow shock if the shock Alfvén number A is less than 1, a fast shock if A is greater than 1. In coronal space, the Alfvén speed is on the order of 1000 km/s. If a forward MHD shock forms preceding the compressed ambient plasma shell associated with the CME, the shock Alfvén number can be less than 1 and the shock can be a forward slow shock.

The plasma density ρ , the thermal pressure p , and the total pressure p^* (the sum of the thermal

and the magnetic pressures) all increase across an MHD shock. The magnetic field and the shock angle decrease across a slow shock and increase across a fast shock. The change in shock angle across an MHD shock may be called the deflection angle. Edmiston and Kennel [1986] and Whang [1988] have studied the slow shock solutions for the jumps of physical properties as functions of various combinations of dimensionless parameters.

The plasma β value plays an interesting role in the jumps of thermodynamic properties across slow shocks. In coronal space where the β value of the solar wind is on the order of 0.1 or less, the discontinuity in thermodynamic properties across a slow shock may vary over a wide range of magnitudes. On the other hand, near 1 AU where the average β value of the solar wind is on the order of 1, the jump in thermodynamic properties across a slow shock becomes very small. The jump in field-related properties behaves quite differently. At any given values of β , in the domain of solutions for slow shocks the magnetic field ratio B_2/B_1 changes over a whole range, from 0 to 1, and the deflection angle also changes over a whole range, $0 \leq \delta \leq 90^\circ$. A shock may be called a weak shock wave only when the discontinuity in every quantity is small. A slow shock with small discontinuity in thermodynamic properties is not necessarily a weak shock. However, when the discontinuities in thermodynamic properties are small, the identification of a slow shock from plasma observations becomes difficult.

2. Forward-Reverse Shock Pairs

We would like to investigate the dynamic interaction between the coronal mass ejecta and the ambient solar wind. Reference should be made to an excellent review of recent work on CMEs by Kahler [1987]. The association between interplanetary shocks and CMEs has been clearly demonstrated using shocks detected at Helios 1 and CMEs observed from Solwind coronagraph [Sheeley et al., 1985]. With very few exceptions, interplanetary shocks are produced by major CMEs and are confined in latitude to within 15° of the angular extents of the CMEs measured at $10 R_\odot$.

The number of slow shocks observed in interplanetary space is very small. Chao and Olbert [1970] have identified two forward slow shocks. Burlaga and Chao [1971] found a reverse and a forward slow shock. Richter et al. [1985] reported a very certain identification of a forward slow shock.

We may call the ejected material the CME plasma which is separated from the solar wind plasma in the background corona by a tangential discontinuity. The large momentum of the high-speed mass ejecta exerts an excessive pressure on the ambient plasma shell in a narrow region in front of the CME. This causes a sudden increase

Copyright 1988 by the American Geophysical Union.

Paper number 8A9491.

0148-0227/88/008A-9491\$02.00

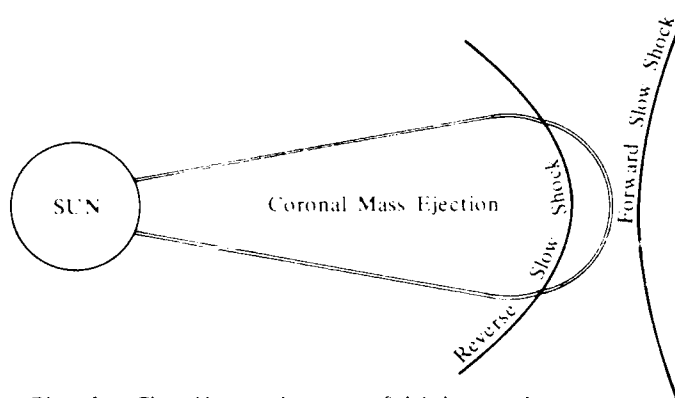


Fig. 1. The direct impact of high-speed mass ejecta on the ambient solar wind compresses the plasma near the top of CME on both sides of the tangential discontinuity. This interaction produces a forward shock preceding the CME and a reverse shock in the CME plasma closely behind the leading edge.

in the pressure of the plasma shell. When the velocity at the front of the CME relative to the ambient solar wind exceeds the local magnetoacoustic speed, a forward MHD shock may form preceding the compressed ambient plasma shell. The nose of the shock should be at some standoff distance from the top of the CME. The shock is a forward slow shock if the normal component of the relative shock velocity U_n is greater than the slow mode magnetoacoustic speed but less than $a \cos \theta$. The shock is a fast shock if U_n is greater than both the fast-mode magnetoacoustic speed and $a \cos \theta$.

Recently, Hundhausen et al. [1987] studied CMEs observed from the coronagraphs aboard Skylab and on the Solar Maximum Mission satellite. The observed flattening of the tops of some mass ejection loops suggests the possible existence of traveling forward slow shocks immediately in front of some CMEs. Their study of the observed speeds for the outward motion of CMEs shows that the speed at which a CME is overtaking the ambient coronal plasma is less than the Alfvén speed but greater than the sound speed for many (probably most) observed CMEs. This also supports the possible existence of forward slow shocks.

In response to the large pressure in the compressed ambient plasma shell, the CME plasma immediately behind the tangential discontinuity is also decelerated, compressed and heated. This compressed CME plasma is confined in a narrow leading edge region bounded by the tangential discontinuity on the forward side and by a pressure front on the reverse side. The pressure front propagates in the reverse direction relative to the motion of the ejected material. Due to greater wave propagation speed on the side of the compressed CME plasma at the pressure front, the pressure profile and the flow speed profile steepen to form a reverse MHD shock as the CME moves outward from the Sun.

The ejected CME plasma carrying a strong magnetic field is a low- β plasma in which the slow mode magnetoacoustic speed C_s is much less than the Alfvén speed a . The reverse shock associated with CME can be a slow shock if the normal component of the relative shock speed U_n

is greater than C_s but less than $a \cos \theta$. Since U is the relative shock speed the above condition does not imply that the absolute velocity of the ejecta is low. We do not yet have a theory to explain why the pressure front steepens to form a slow shock rather than a fast shock in a low- β plasma in the coronal environment. The possible observation of forward slow shocks associated with CME by Hundhausen et al. [1987] provides an observational support for such a hypothesis. On this basis we estimate that the reverse shock can be a slow shock whether the forward one is a slow-mode or a fast-mode shock.

Figure 1 shows a sketch of the forward-reverse shock pair associated with CMEs in the early phase of the shock pair. A large portion of the shock surface inside the ejecta is quasi-perpendicular shock with the shock angle θ slightly less than or equal 90° . Edmiston and Kennel [1996] and Whang [1987, 1988] showed that slow shocks with large shock angle θ exist at all β values. In the limit of $\theta = 90^\circ$, the deflection angle δ approaches zero and the ratio of the total pressure p_2/p_1 approaches unity. The thermal pressure always increases and the magnetic pressure always decreases across a slow shock, but the two effects cancel out in the limiting case of $\theta = 90^\circ$. Because the total pressure p^* must be continuous at every point across a tangential discontinuity, the jump in p^* across the reverse slow shock must be maintained across the boundary surface of the CME plasma as the shock intersects with the boundary. This requires that the reverse shock must extend to the solar wind outside of the tangential discontinuity. The dynamical equilibrium of the solar wind flow field in the neighborhood of the ejecta has to be maintained in such a way that this boundary condition be satisfied. In Figure 2, we use an r - t diagram to demonstrate the forward-reverse shock pair near the top of a CME. As mass ejections sweep through the corona, a tangential discontinuity separates the CME plasma from the solar wind in the background corona, a reverse slow shock propagates in the region of CME plasma, while a forward shock propagates in the solar wind ahead of the CME. The dotted lines indicate the paths of fluid elements.

Numerical simulations have been used to demonstrate the possible existence of forward shock in association with flares by Hundhausen and Gentry [1969] and the possible existence of forward-reverse MHD shock pairs by Steinolfson et al. [1975] and Whang [1984]. The evolution of a corotating stream also leads to the formation of a corotating forward-reverse shock pair [Dessler and Fejer, 1963; Sonnett and Colburn, 1965; Whang and Chien, 1981]. The region bounded by a corotating shock pair is known as a corotating interaction region (CIR). Evolution of corotating shock pairs and CIR has been very well studied in the literature (see a review by Burlaga [1988] and references therein). Corotating shock pairs begin to form at near 1 AU in interplanetary space. The shocks are weak near 1 AU and they become quite strong in the outer heliosphere. The direction of a corotating stream makes a spiral angle with the heliocentric radial direction. This effect substantially reduces the normal impact of the momentum of a high-speed stream on preceding solar wind streams. In contrast, the coronal mass ejecta can exert a direct impact on

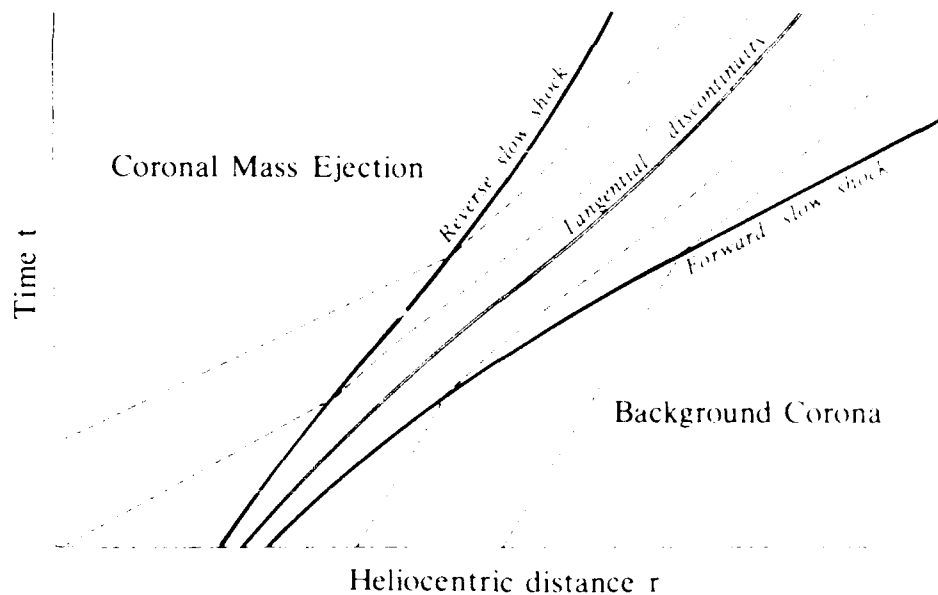


Fig. 2. As mass ejections sweep through the corona, a tangential discontinuity separates the CME plasma from the solar wind in the background corona, a reverse slow shock propagates in the region of CME plasma, while a forward shock propagates in the solar wind ahead of the CME. The dotted lines indicate the paths of fluid elements.

the ambient solar wind. The plasma pressure can build up very rapidly near the top of a CME on both sides of the tangential discontinuity which separates the CME plasma from the ambient solar wind plasma. Thus the forward-reverse shock pairs associated with CMEs can form very rapidly in coronal space.

3. Interplanetary Evolution of CME-Associated Shock Pairs

Two important evolutions of the shock pairs associated with CMEs may occur in interplanetary space. First, a CME loop may disconnect from the Sun to form a closed magnetic structure. The disconnected bubble is believed to manifest as a magnetic cloud in interplanetary space. Second, slow shocks may convert to fast shocks. As a result, we picture the interplanetary consequence of some CMEs as a magnetic cloud accompanied by a shock pair: a forward fast shock precedes the cloud and a reverse fast shock either within or behind the cloud.

MacQueen [1980] studied the average CME occurrence rate and the magnetic flux present in each CME. He suggested that CMEs do not carry out a distended field very far to interplanetary space, but rather are subject to a reconnection process. He proposed that CME loops must magnetically disconnect from the Sun and form a closed magnetic structure. The disconnected bubble continues outward into interplanetary space.

Burlaga et al. [1981] analyzed the magnetic field configuration behind three shocks. They found a systematic configuration of the magnetic field and called it the magnetic cloud. A magnetic cloud is identified as an interplanetary structure in which the magnetic field strength is higher than average, the magnetic field direction rotates monotonically through a large angle, the temperature is low, and the plasma β is

significantly lower than 1. Burlaga and Behannon [1982] showed that clouds persisted to the distances of 2 to 4 AU and estimated that the front and rear of a cloud expand at a speed of the order of half the Alfvén speed. Klein and Burlaga [1982] identified 45 clouds in interplanetary data obtained near 1 AU between 1967 and 1978. About one third of them are preceded by a shock, and these clouds appear to be moving faster than the ambient solar wind ahead. They compared the physical properties of magnetic clouds with those of CMEs and suggested an association of some clouds with disconnected magnetic structures of CMEs. A good case of an association between a CME observed by Solwind and a magnetic cloud observed at 0.54 AU by Helios 1 two days later was presented by Burlaga et al. [1982].

The Alfvén speed decreases at increasing heliocentric distance in the inner solar wind. As a forward or reverse slow shock travels outward from the Sun, the decrease in the Alfvén speed causes the shock Alfvén number to become greater than 1 at increasing heliocentric distances and the shock evolves from a slow shock into a fast shock. The transition of a forward slow shock which precedes a CME to a forward fast shock has been discussed by Wang [1987]. The reverse slow shock may also evolve into a reverse fast shock. The onset for the transition of reverse slow shocks may take place at the tangential discontinuity which is the boundary between the CME plasma and the ambient solar wind, inside the boundary, or outside the boundary.

Occurrence of Transition Inside or Outside of CMEs

If the onset of transition of reverse shocks occurs either inside or outside of the boundary tangential surface, the process should be similar to that for the transition of forward shocks.

Transition of a reverse slow shock to a reverse fast shock

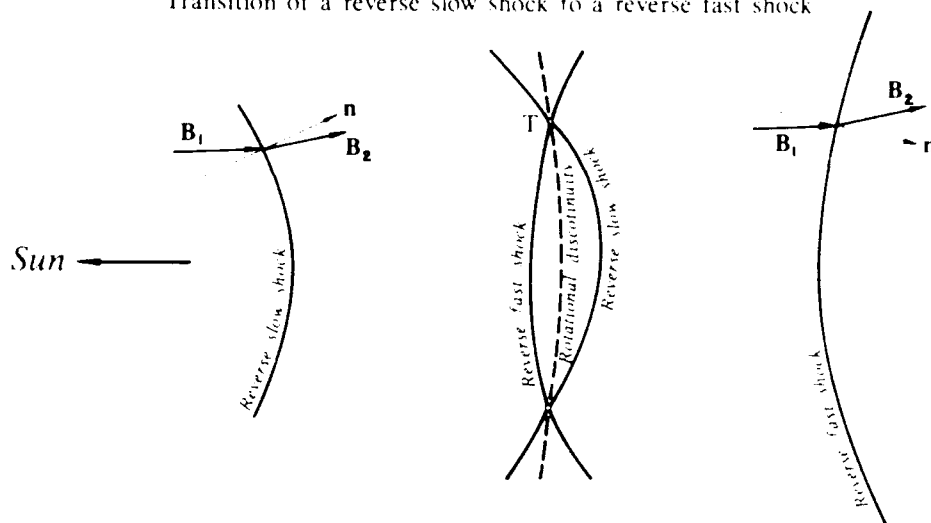


Fig. 3 This figure depicts the process for the transition of a reverse slow shock into a reverse fast shock. The normal vectors \mathbf{n} point in the direction of plasma flow relative to the shock surface.

Figure 3 depicts the transition of a reverse slow shock to a reverse fast shock. The vector \mathbf{n} denotes the normal direction pointing in the direction of plasma flow relative to the shock surface. The solar wind plasma enters a shock from its front side. The front side (the upstream side) of a reverse shock is the side closer to the Sun and the back side (the downstream side) is the side further away from the Sun. The surface of a reverse slow shock has a bow-shaped surface with its nose facing away from the Sun and the surface of a reverse fast shock has a bow-shaped surface with its nose facing the Sun.

As the reverse slow shock moves outwards from the Sun, the decrease in the Alfvén speed causes the shock Alfvén number to reach 1 near the nose of the shock surface, the transition from a reverse slow shock to a reverse fast shock begins to take place at a point of the shock surface where the shock angle equals 0° . At the onset of the transition process the reverse slow shock smoothly converts to a system consisting of a reverse slow shock, a very weak reverse rotational discontinuity (an Alfvén wave), and a very weak reverse fast shock (a fast MHD wave). A smooth conversion requires that at the onset of transition the three discontinuity surfaces (the slow shock, the weak rotational discontinuity and the weak fast shock) move at the same speed. Whang (1987, 1988) shows that the onset of transition must occur in the region of interplanetary space where $\beta < 2/\gamma$ or 1.7.

During the transition, the system consists of a reverse slow shock, a reverse fast shock, and a reverse rotational discontinuity. The three surfaces of discontinuity intersect along a closed transition line. As the system moves outward from the Sun, the transition line moves laterally across the field lines, the area enclosed by the closed loop of the transition line expands continuously, the fast shock grows stronger, and the slow shock becomes weaker. Eventually, the reverse slow shock diminishes and the entire system evolves into a reverse fast shock.

The fast shock of a forward or reverse transition system is a near switch-on shock, across which small random fluctuations in plasma flow and magnetic fields on the front side of the shock are considerably amplified. The flow becomes very turbulent behind nearly switch-on shocks. Therefore during the transition, the amplitude of fluctuations in flow velocity and magnetic fields are large in the turbulent region behind the fast shock (Whang, 1988).

Kennel et al. (1984a, b) reported a sequence of events observed from ISEE 1 and 3 that seems to resemble the forward transition system. On November 12, 1978, the passage over the ISEE spacecraft of a high-speed, quasi-parallel, interplanetary forward fast shock with $U_{n1} = 240 \text{ km s}^{-1}$, $\theta_1 = 41^\circ$, $a_1 = 160 \text{ km s}^{-1}$ and $\beta_1 = 1.14$. The shock is followed by a strong magnetic field rotation at approximately $40 R_E$ downstream of the shock, and an extended region of intense MHD turbulence between the shock and the magnetic field rotation. They reported that the shock was probably associated with the pair of flares beginning at 0048 and 0113 UT on November 10, 1978.

Occurrence of Transition at the Boundary of CMEs

Figure 1 shows that a reverse slow shock in the CME plasma extend to the ambient solar wind outside of the tangential discontinuity surface, if the relative flow velocity across the tangential discontinuity is less than the Alfvén speeds on both sides, the flow satisfies the criterion of Kelvin-Helmholtz stability. The flow velocity and the Alfvén speed are discontinuous across a tangential discontinuity. But the total pressure p^* must be continuous across a tangential discontinuity and the magnetic field vectors and the relative flow velocities on both sides must be parallel to the tangential discontinuity surface. As the shock angle decreases across the reverse slow shock inside the CME, the boundary surface must deflect by a small angle at the location where the reverse

slow shock intersects the tangential discontinuity. The flow pattern near the deflection point of the boundary in the ambient solar wind may consist of a reverse slow shock, a reverse rotational discontinuity, and a reverse fast shock. Depending on the physical properties outside the CME boundary, the slow (fast) shock can be replaced by a continuous centered slow (fast) expansion wave. As the cluster consisting of the cloud and the shock pair moves outward from the Sun, the decrease in the Alfvén speed can cause a possible conversion of the pattern for shocks and discontinuities near the deflection point of the boundary in the ambient solar wind from the pattern of a reverse slow followed by a reverse rotational discontinuity to that of a reverse fast shock preceded by a reverse rotational discontinuity.

4 Conclusions

For some coronal mass ejections (CMEs), the direct impact of the high-speed mass ejecta on the ambient solar wind can substantially compress the plasma near the leading edge of the CME on both sides of the tangential discontinuity which separates the CME plasma from the ambient solar wind plasma. This interaction can produce a forward shock preceding the CME and a reverse slow shock in the CME plasma closely behind the leading edge. As the forward-reverse shock pair moves outward in interplanetary space, it evolves into a pair of fast shocks. If the magnetic clouds are indeed the interplanetary manifestations of the disconnected magnetic structures of CMEs, then the reverse shock propagates within the magnetic cloud as the cloud moves outward from the Sun. Eventually, the reverse shock exits the cloud to become detached from the magnetic cloud. Then both the forward and the reverse shocks propagate in the ambient solar wind as shown in Figure 4. If this picture is correct, the interplanetary signature of some CMEs at large heliocentric distances may consist of a magnetic cloud wrapped around by an interaction region, which in turn is bounded by a pair of fast shocks. The solar wind plasma continuously adds to the interaction region

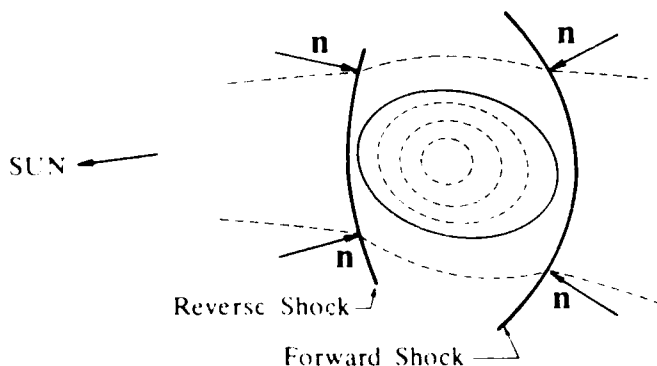


Fig. 4. The reverse shock propagates within the cloud as it moves outward from the Sun. Eventually, the reverse shock exits the cloud to become detached from the magnetic cloud. The cloud is now wrapped around by an interaction region which is itself bound by a pair of forward reverse fast shocks.

across the shocks as the system moves away from the Sun.

Klein and Burlaga [1982] reported that about one third of clouds identified near 1 AU between 1967 and 1978 are preceded by a shock. There are two examples involving the observation of a reverse shock and a magnetic cloud. R. P. Lepping et al. (private communication, 1988) have observed one; their report will soon be ready for journal publication. Another event involving a reverse shock and a magnetic cloud was observed on August, 1982, from Voyager 2 [Burlaga et al., 1985]. The observed cloud remained stable out to 10.3 AU after a propagation time of approximately a month. The cloud had a dimension of the order of 1 AU and was preceded by two shocks and an interface and followed by a reverse fast shock at about 0.1 AU behind the cloud. This observation probably explains that for a long-lived cloud, the reverse shock had enough time to propagate through the cloud, exited the rear of the cloud, and appeared closely behind the cloud.

Acknowledgments. The author thanks K. W. Behannon, L. F. Burlaga, S. Kahler, and C. F. Kennel for useful discussions of this topic, and L. F. Burlaga for his comments on the manuscript. This work was supported by the Air Force Office of Scientific Research under contract AF-160, and by the Atmospheric Sciences Section of the National Science Foundation under grant ATM-8614990.

The Editor thanks R. S. Steinolfson and another referee for their assistance in evaluating this paper.

References

- Burlaga, L. F., Interaction regions in the distant solar wind, *Proceedings of Solar Wind Six*, NCAR Tech. Note, in press, 1988.
- Burlaga, L. F., and K. W. Behannon, Magnetic clouds: Voyager observations between 7 and 4 AU, *Sol. Phys.*, **81**, 181, 1982.
- Burlaga, L. F., and J. K. Chao, Reverse and forward slow shocks in the solar wind, *J. Geophys. Res.*, **76**, 1516, 1971.
- Burlaga, L. F., E. Sittler, F. Mariani, and B. Schwenn, Magnetic loop behind an interplanetary shock: Voyager, Helios and IMP 8 observations, *J. Geophys. Res.*, **86**, 6577, 1981.
- Burlaga, L. F., I. Klein, N. R. Sheeley Jr., D. J. Michels, R. A. Howard, M. L. Koomen, R. Schwenn, and H. Rosenbauer, A magnetic cloud and a coronal mass ejection, *Geophys. Res. Lett.*, **9**, 1317, 1982.
- Burlaga, L. F., F. B. McDonald, M. L. Goldstein, and A. J. Lazarus, Cosmic ray modulation and turbulent interaction regions near 11 AU, *J. Geophys. Res.*, **90**, 11,027, 1985.
- Chao, J. K., and S. Olbert, Observation of slow shocks in interplanetary space, *J. Geophys. Res.*, **75**, 6394, 1970.
- Dessler, A. J., and J. A. Feder, Interpretation of Kp index and M region geomagnetic storms, *Planet. Space Sci.*, **11**, 205, 1963.
- Edmiston, J. P., and C. F. Kennel, A parametric study of slow shock Rankine-Hugoniot solutions and critical Mach numbers, *J. Geophys. Res.*, **91**, 1361, 1986.

- Hundhausen, A. J., and R. A. Gentry, Numerical simulation of flare-generated disturbances in the solar wind, J. Geophys. Res., 74, 2908, 1969.
- Hundhausen, A. J., T. E. Holzer, and B. C. Low, Do slow shocks precede some coronal mass ejections?, J. Geophys. Res., 92, 11,173, 1987.
- Kahler, S., Coronal mass ejections, Rev. Geophys., 25, 663, 1987.
- Kennel, C. F., F. L. Scarf, F. V. Coroniti, C. T. Russell, K. P. Wenzel, T. R. Sanderson, P. Van Nes, W. C. Feldman, G. K. Parks, E. J. Smith, B. T. Tsurutani, F. S. Mozer, M. Temerin, R. R. Anderson, J. D. Scudder, and M. Scholer, Plasma and energetic particle structure upstream of a quasi-parallel interplanetary shock, J. Geophys. Res., 89, 5419, 1984a.
- Kennel, C. F., J. P. Edmiston, F. L. Scarf, F. V. Coroniti, C. T. Russell, E. J. Smith, B. T. Tsurutani, J. D. Scudder, and W. C. Feldman, Structure of the November 12, 1978, quasi-parallel interplanetary shock, J. Geophys. Res., 89, 5436, 1984b.
- Klein, L. W., and L. F. Burlaga, Interplanetary magnetic clouds at 1 AU, J. Geophys. Res., 87, 613, 1982.
- MacQueen, R. M., Coronal transients: A summary, Philos. Trans. R. Soc. London, Sec. A, 297, 605, 1980.
- Richter, A. K., H. Rosenbauer, F. M. Neubauer, and N. G. Ptitsyna, Solar wind observations associated with a slow-forward shock wave at 0.31 AU, J. Geophys. Res., 90, 7581, 1985.
- Sheeley, N. R., Jr., R. A. Howard, M. J. Koomen, D. J. Michels, R. Schwenn, K. H. Mulhauser, and H. Rosenbauer, Coronal mass ejections and interplanetary shocks, J. Geophys. Res., 90, 163, 1985.
- Sonnett, C. P., and D. S. Colburn, The Si^{+} - Si^{+} pair and interplanetary forward reverse shock ensembles, Planet. Space Sci., 13, 675, 1965.
- Steinolfson, R. S., M. Dryer, and Y. Nakagawa, Numerical MHD simulation of interplanetary shock pairs, J. Geophys. Res., 80, 1223, 1975.
- Whang, Y. C., The forward-reverse shock pair at large heliocentric distances, J. Geophys. Res., 89, 7367, 1984.
- Whang, Y. C., Slow shocks and their transition to fast shocks in the inner solar wind, J. Geophys. Res., 92, 4349, 1987.
- Whang, Y. C., Evolution of interplanetary slow shocks, J. Geophys. Res., 93, 251, 1988.
- Whang, Y. C., and T. H. Chien, Magnetohydrodynamic interaction of solar wind streams, J. Geophys. Res., 86, 3263, 1981.

Y. C. Whang, Department of Mechanical Engineering, Catholic University of America, Washington, DC 20064.

(Received January 12, 1988;
revised February 16, 1988;
accepted February 25, 1988.)

CME ASSOCIATED FORWARD-REVERSE SHOCK PAIRS

Y. C. Whang

*Department of Mechanical Engineering, Catholic University of America,
Washington, DC 20064, U.S.A.*

ABSTRACT

For some coronal mass ejections (CMEs), their interaction with the ambient solar wind can produce a forward-reverse shock pair. The high-speed mass ejecta compresses the plasma near the top of the CME on both sides of the tangential discontinuity which separates the CME plasma from the ambient solar wind plasma. The front of the compressed CME plasma propagates in the reverse direction relative to the ejecta flow, it may steepen to form a reverse slow shock. The front of the compressed solar wind plasma also propagates in the forward direction relative to the ambient solar wind and it may steepen to form a forward shock. The forward-reverse shock pair associated with CMEs moves outward in interplanetary space and evolves into a pair of fast shocks. The interplanetary manifestation of some CMEs is pictured as a magnetic cloud accompanied by a shock pair: a forward shock precedes the cloud and a reverse shock either within or behind the cloud.

INTRODUCTION

The solutions of MHD shocks [1] may be expressed as functions of three dimensionless upstream conditions: the shock Alfvén number based on the relative shock speed $A = U_n/(a \cos \theta)$, the shock angle θ , and the plasma β value. (Here U_n is the normal component of the relative shock speed, a the Alfvén speed, θ the acute angle between the shock normal and the magnetic field, and β the ratio of the thermal pressure p to the magnetic pressure $B^2/8\pi$.) A shock is a slow shock if the shock Alfvén number A is less than 1 and is a fast shock if A is greater than 1. The magnetic field and the shock angle decrease across a slow shock, they increase across a fast shock.

The association between interplanetary shocks and CMEs has been clearly demonstrated using shocks detected at Helios 1 and CMEs observed from Solwind coronagraph [2]. In 1986, Whang first suggested the possible existence of forward slow shocks preceding some CMEs and the transition of slow shocks to fast shocks [1,3]. The theory was reported at the XXVI COSPAR Meeting at Toulouse on July 1986. Whang explained that when the speed of ejected CME material relative to the ambient solar wind exceeds the local magnetoacoustic speed, an MHD shock front forms at the leading edge of the compressed ambient plasma shell. In coronal space, the Alfvén speed is of the order of 1000 km/s. If a forward MHD shock forms preceding the compressed ambient plasma shell associated with the CME, the shock Alfvén number can be less than 1 and the shock can be a forward slow shock.

Whang also discussed the large scale geometries of forward slow and fast shocks, and the transition of slow shocks to fast shocks in the inner solar wind. The large-scale global surface of a forward slow shock should have a bow-shaped surface with its nose facing the sun because the slow mode MHD waves and MHD shocks are upstream-tilted. The relative shock speed varies from point to point on the curved surface of a 3-D shock. The slow shock is relatively stronger at the nose. The shock becomes weaker on the flank and asymptotically

shock.

fast shock of a transition system is a near switch-on shock across which small random fluctuations in plasma flow and magnetic fields on the front side of the shock are considerably amplified. The flow becomes very turbulent behind nearly switch-on shocks. Therefore, during the transition, the amplitude of fluctuations in flow velocity and magnetic fields are large in the turbulent region behind the fast shock.

Kennel et al. /6,7/ reported the observation of a rotational discontinuity preceded by a forward shock from ISEE 1 and 3. On 12 November 1978, the passage over the ISEE spacecraft of a high speed, quasi-parallel, interplanetary forward fast shock with $U_{n1} \approx 240 \text{ km s}^{-1}$, $\theta_1 = 41^\circ$, $a_1 \approx 160 \text{ km s}^{-1}$ and $\beta_1 \approx 1.14$. The shock was probably associated with a pair of flares which occurred some 48 hours earlier. The shock is followed by a strong magnetic field rotation at approximately $40 R_E$ downstream of the shock, and an extended region of intense MHD turbulence between the shock and the magnetic field rotation. This sequence of events observed from ISEE 1 and 3 seems to resemble a forward transition system.

INTERPLANETARY MANIFESTATION

Two important evolutions of the shock pairs associated with CMEs may occur in interplanetary space. First, a CME loop may disconnect from the sun to form a closed magnetic structure. The disconnected bubble is believed to manifest as a magnetic cloud in interplanetary space. Second, for some coronal mass ejections (CMEs), the direct impact of the high-speed mass ejecta on the ambient solar wind can produce a forward shock preceding the CME and a reverse slow shock in the CME plasma closely behind the leading edge. As the forward-reverse shock pair moves outwards in interplanetary space, they evolve into a pair of fast shocks.

MacQueen /8/ suggested that CMEs do not carry out distended field very far to interplanetary space, but rather are subject to a reconnection process. He proposed that CME loops must magnetically disconnect from the sun and form a closed magnetic structure. The disconnected bubble continues outward into interplanetary space.

If the magnetic clouds are indeed the interplanetary manifestations of the disconnected magnetic structures of CMEs then the reverse shock propagates within the magnetic cloud as the cloud moves outward from the sun. Eventually, the reverse shock exits the cloud to become detached from the magnetic cloud as shown in Figure 3. The cloud is now wrapped around by an interaction region which is itself bound by a pair of forward-reverse fast shocks.

Burlaga and his coworkers /9-11/ identified a magnetic cloud as an interplanetary structure in which the magnetic field strength is higher than average, the magnetic field direction rotates monotonically through a large angle, the temperature is low, and the plasma β is significantly lower than 1. Clouds may persist to the heliocentric distances of 2 to 4 AU. They also suggested an association of some clouds with disconnected magnetic structures of

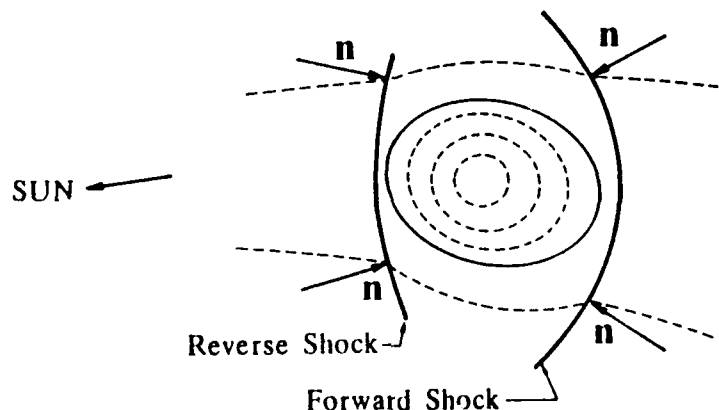


Fig. 3. The reverse shock propagates within the cloud as it moves outward from the Sun. Eventually, the reverse shock exits the cloud to become detached from the magnetic cloud. The cloud is now wrapped around by an interaction region which is itself bound by a pair of

forward-reverse fast shocks.

CMEs. Klein and Burlaga /12/ reported that about one third of clouds identified near 1 AU between 1967 and 1978 were preceded by a shock.

Two recent papers reported the observations of CME associated forward-reverse shock pairs at near 1 AU. Lepping, Ipavich and Burlaga /13/ reported that a large magnetic cloud accompanied by a shock pair was observed on October 31 and November 1 of 1972 from IMP 7. The plasma, magnetic field and energetic particle data observed a forward shock wave followed by a large tangential discontinuity and a reverse shock. The tangential discontinuity was the forward boundary of the magnetic cloud. The reverse shock was within the cloud. The flow system was associated with a unusually longlasting solar flare which occurred some 49 hours earlier. Gosling et al. /14/ reported that they have identified two CME associated forward-reverse shock pairs at 1 AU using plasma and magnetic field data from ISEE 3 for the interval from August 1978 through February 1980. The shock pairs were closely associated with the propagation of transient disturbances. Strong bidirectional electron heat flux events, which they identified as the CME driving the shocks, were detected during both of these disturbances. In the stronger of the two disturbances the reverse shock was found within the CME and was separated from the forward shock by ≈ 0.2 AU. In the weaker of the two disturbances the reverse shock had propagated entirely through the CME and trailed the forward shock by 0.3 - 0.4 AU.

Burlaga et al. /15/ reported another event observed at 10.3 AU from Voyager 2 on August 1982 involving forward, reverse shock waves and a magnetic cloud on August, 1982 from Voyager 2. The observed cloud remained stable out to 10.3 AU after a propagation time of approximately a month. The cloud had a dimension of the order of 1 AU and was preceded by two shocks and an interface and followed by a reverse fast shock at about 0.1 AU behind the cloud. This observation indicates that for a long-lived cloud, the reverse shock had enough time to propagate through the cloud, exited the rear of the cloud, and appeared closely behind the cloud.

ACKNOWLEDGMENTS

This work was supported by the Air Force Office of Scientific Research under contract 86-160.

REFERENCES

1. Y. C. Whang, Slow shocks and their transition to fast shocks in the inner solar wind, J. Geophys. Res., 92, 4349, (1987).
2. N. R. Sheeley, Jr., R. A. Howard, M. J. Koomen, D. J. Michels, R. Schwenn, K. H. Muhlhauser, and H. Rosenbauer, Coronal mass ejections and interplanetary shocks, J. Geophys. Res., 90, 163, (1985).
3. Y. C. Whang, Transition of traveling interplanetary slow shock to fast shock, Eos Trans. AGU, 67, 327, (1986).
4. A. J. Hundhausen, T. E. Holzer, and B. C. Low, Do slow shocks precede some coronal mass ejections?, J. Geophys. Res., 92, 11,173, (1987).
5. Y. C. Whang, Forward-Reverse Shock Pairs Associated with Coronal Mass Ejections, J. Geophys. Res., 93, 5897, (1988).
6. C. F. Kennel, F. L. Scarf, F. V. Coroniti, C. T. Russell, K. P. Wenzel, T. R. Sanderson, P. Van Nes, W. C. Feldman, G. K. Parks, E. J. Smith, B. T. Tsurutani, F. S. Mozer, M. Temerin, R. R. Anderson, J. D. Scudder, and M. Scholer, Plasma and energetic particle structure upstream of a quasi-parallel interplanetary shock, J. Geophys. Res., 89, 5419, (1984).
7. C. F. Kennel, J. P. Edmiston, F. L. Scarf, F. V. Coroniti, C. T. Russell, E. J. Smith, B. T. Tsurutani, J. D. Scudder, and W. C. Feldman, Structure of the November 12, 1978, quasi-parallel interplanetary shock, J. Geophys. Res., 89, 5436, (1984).
8. R. M. MacQueen, Coronal transients: A summary, Philos. Trans. R. Soc. London, Sec. A, 297, 605, (1980).
9. L. F. Burlaga, E. Sittler, F. Mariani, and R. Schwenn, Magnetic loop behind an interplanetary shock: Voyager, Helios and IMP 8 observations, J. Geophys. Res., 86, 6673.

(1981).

10. L. F. Burlaga and K. W. Behannon, Magnetic clouds: Voyager observations between 2 and 4 AU, Sol. Phys., 81, 181, (1982).
11. L. F. Burlaga, L. Klein, N. R. Sheeley, Jr., D. J. Michels, R. A. Howard, M. J. Koomen, R. Schwenn, and H. Rosenbauer, A magnetic cloud and a coronal mass ejection, Geophys. Res. Lett., 9, 1317, (1982).
12. L. W. Klein and L. F. Burlaga, Interplanetary magnetic clouds at 1 au, J. Geophys. Res., 87, 613, (1982).
13. R. P. Lepping, F. M. Ipavich, L. F. Burlaga, A flare-associated shock pair at 1 AU and related phenomena, (1988).
14. J. T. Gosling, S. J. Bame, E. J. Smith, and M. E. Burton, Forward-reverse shock pairs associated with transient disturbances in the solar wind at 1 AU, J. Geophys. Res., (1988).
15. L. F. Burlaga, F. B. McDonald, M. I. Goldstein, and A. J. Lazarus, Cosmic ray modulation and turbulent interaction regions near 11 AU, J. Geophys. Res., 90, 12,027, (1985).